

AD 689865

Technical Progress Report 69-1  
Semiannual

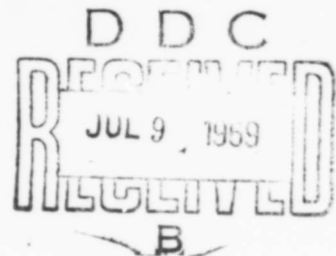
September 16, 1968 to  
March 15, 1969

SENSITIVITY FUNDAMENTALS

Prepared for:

Office of Naval Research  
Department of the Navy  
Washington, D.C. 20360

Contract Nonr 3760(00)



This document has been approved  
for public release and sale; its  
distribution is unlimited



**STANFORD RESEARCH INSTITUTE**  
Menlo Park, California 94025 • U.S.A.

Reproduced by the  
CLEARINGHOUSE  
for Federal Scientific & Technical  
Information Springfield Va. 22151



STANFORD RESEARCH INSTITUTE  
Menlo Park, California 94025 · U.S.A.

May 31, 1969

Technical Progress Report 69-1 Semiannual

September 16, 1968 to  
March 15, 1969

SENSITIVITY FUNDAMENTALS

Prepared for:

Office of Naval Research  
Department of the Navy  
Washington, D.C. 20360

Contract Nonr 3760(00)

SRI Project PRU-4051

Approved: M. E. Hill, Director  
Physical Sciences (Chemistry)

Marjorie W. Evans, Executive Director  
Physical Sciences Division

Reproduction in whole  
or in part is permitted  
for any purpose of the  
United States Government.

Copy No. 15

## PREFACE

This project is the responsibility of the Chemistry Program of the Physical Sciences Division of Stanford Research Institute, in cooperation with the Physics and Chemistry of Fluids Program. Project organization and principal contributors to the technical work are:

<b>Program Manager:</b>	M. E. Hill
<b>Low-Velocity Detonation:</b>	R. W. Woolfolk H. R. Bredfeldt D. Tegg
<b>Physics and Chemistry of Detonation:</b>	R. Shaw M. Cowperthwaite
<b>Kinetics and Mechanisms of Thermal Decomposition:</b>	D. S. Ross D. Tegg M. E. Hill

## SUMMARY

Under the sponsorship of the Office of Naval Research, Stanford Research Institute is studying the following fundamental sensitivity properties of difluoramino compounds:

1. The low-velocity detonation (LVD) wave characteristics of the liquid phase.
2. The relation of shock sensitivity and failure diameter to the flow and the chemical reaction rate behind the shock front,
3. The mechanism and kinetics of thermal decomposition of the compounds in the gas phase.

The compounds chosen for this study are as simple as possible structurally, but at the same time they have physical properties that permit their use in each phase of the study. The model compounds are the bis difluoramino and tris difluoramino isomers of the propane series--primarily 1,2-, 1,3-, 1,1-, and 2,2-bis(difluoramino)propane (1,2-, 1,3-, 1,1-, and 2,2-DP); 1,2-bis(difluoramino)-2-methyl propane (IBA); 2,3-bis(difluoramino)butane, (2,3-DB) in meso and *dl* forms; 1,2,2-tris(difluoramino)propane (1,2,2-TP); and 2,3,3-tris(difluoramino)-butane (2,3,3-TB). These compounds are being used so that the results from each experimental technique can be interrelated without having to account for effects caused by different functional groups, amount of carbon content, and chain branching. Through the use of isomers, structural effects on the results from a particular technique can be determined--for example, the differences in the effect of vicinal and geminate difluoramino groups on the ease of initiation and on the environmental stability of compounds containing them. A similar approach has begun with isomeric nitro compounds.

### Low-Velocity Detonation

The shock wave interactions that can lead to the initiation of low-velocity detonations (LVD) are examined with particular emphasis

on cavitation. The two forms of cavitation, gas inclusion and pure vaporization, are discussed. The latter's relationship to the shock-wave interactions in the LVD gap sensitivity tests is examined. We believe that pure vaporization cavitation, which cannot be removed by degassing, is present under gap test conditions. Experimental studies in the gap test arrangement show the presence of cavitation in qualitative agreement with theoretical prediction.

The "universal Hugoniot" for liquids has been reevaluated using a temperature correction for the sonic velocity,  $c_0$ . The new equation is improved slightly over the one formerly used. This concluded the effort in this area.

A trace dye method for following the flow field behind a shock wave was studied. We concluded that this method was not suitable at present for our studies and work on it will be discontinued.

Experiments on the effect of confinement wall thickness on the LVD gap sensitivity are discussed and preliminary charge diameter studies are reported. A summary of the effects of confinement on the LVD gap sensitivity is presented.

Some of the physical and chemical properties of liquid explosives are correlated with the LVD gap sensitivity. This correlation is remarkably good considering its simplicity. The evidence that LVD initiation may be a gas phase phenomenon is discussed. This further supports the contention that LVD may be related to the formation of cavities in the liquid explosive.

#### Physics and Chemistry of Detonation

A new method for calculating shock temperatures in liquid explosives has been developed from the Walsh-Christian method for metals. The Walsh-Christian method assumes that  $C_v$  and  $(\partial p/\partial T)_v$  are constant. The basis of the present method is a variational analysis which shows that shock temperature is more sensitive to variations in  $C_v$  than to variations in  $(\partial p/\partial T)_v$ . Thus  $C_v$  is assumed to be a function of temperature and  $(\partial p/\partial T)_v$  is assumed

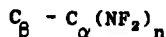
to be constant. It is considered likely that  $C_v$  will increase with temperature due to an increase in the vibrational heat capacity. The simplest assumption is that  $C_v$  of the liquid will increase as  $C_v$  of the ideal gas. This is the basis of the  $C_v(T)$  model.

Shock temperatures of carbon tetrachloride and nitromethane have been calculated using both constant  $C_v$  and  $C_v(T)$ . Shock temperatures for carbon tetrachloride calculated using the  $C_v(T)$  model are in better agreement with experimental brightness temperatures than those calculated using the Walsh-Christian constant  $C_v$  model. Shock temperatures for nitromethane are compared with those of other workers.

Shock temperatures in water were calculated using constant  $C_v$  and  $(\partial p/\partial T)_v$ . The temperatures are about 15% less than those calculated by Rice and Walsh using a model based on constant  $C_p$ . This difference is not regarded as significant compared with the uncertainties in the variation of  $C_v$  and  $C_p$  with temperature and pressure.

#### Kinetics and Mechanisms of Thermal Decomposition

The VLPP studies of all the NF compounds we have had at hand have been completed, and the accumulated data suggest a model of unimolecular decomposition in which the  $NF_2$  compound



is destabilized by both  $\alpha$ - $NF_2$  substitution due to a decrease in  $E_a$ , and by  $\beta$ -alkyl or  $\beta$ - $NF_2$  substitution due to an increase in the A factor. Since both factors are operative in the case of 2,2-DB, it is thermally the least stable NF material we have studied.

A detailed reaction coordinate diagram may be constructed for the system  $F_2N-C-C-NF_2 \rightleftharpoons C=C + N_2F_4$  on the basis of both our work and that by Trotman-Dickenson. It is possible, on the basis of the diagram, to explain the side-products observed in the VLPP of 1,2-DP.

The VLPP of 1-nitropropane has been studied. The products are propylene and presumably HONO, and the  $T_{1/2}$  value is 665°C.

## CONTENTS

PREFACE	111
SUMMARY	v
LIST OF ILLUSTRATIONS	xi
LIST OF TABLES	xiii
GLOSSARY OF COMPOUNDS	xv
I INTRODUCTION	1
II LOW-VELOCITY DETONATION (R. W. Woolfolk and H. R. Bredfeldt)	3
A. Introduction	3
B. Theoretical Studies	4
C. Experimental Studies	12
D. Discussion	20
E. Future Work	25
References	26
III PHYSICS AND CHEMISTRY OF DETONATION (R. Cowperthwaite and R. Shaw)	29
A. Introduction	29
B. The Walsh-Christian Method of Calculating Shock Temperatures	29
C. Variational Analysis of the Walsh-Christian Method (Sensitivity of the Calculated Temperature)	33
D. Effect of Increasing Pressure and Temperature on $\partial p/\partial T)_v$ and $C_v$ .	35
E. The $C_v(T)$ Model	38
F. Results of Temperature Calculations	39
G. Conclusions	42
H. Future Work	42
References	51

<b>IV KINETICS AND MECHANISMS OF THERMAL DECOMPOSITION</b> (David S. Ross and M. E. Hill)	<b>53</b>
<b>A. Introduction</b>	<b>53</b>
<b>B. VLPP of NF Materials</b>	<b>53</b>
<b>C. VLPP of Nitro Materials</b>	<b>59</b>
<b>D. Future Work</b>	<b>62</b>
<b>References</b>	<b>63</b>
<b>APPENDIX: Papers and Presentations Prepared</b>	<b>65</b>
<b>DD Form 1473</b>	<b>67</b>

## ILLUSTRATIONS

### Figure

1	Normalized $U_s - u_p$ plot	7
2	Normalized $p - v/v_0$ plot	8
3	Cavitation in shocked nitromethane	13
4	Unstable LVD in 1,2-DP (0.12 cm tubes)	16
5	Absorption spectra of three compounds	18
6	Absorption spectra of window material and DNEP (colored and colorless)	19
7	Thermodynamic ratio $\Delta H_p/\Delta H_v$ vs. LVD gap sensitivity	23
8	Shock temperature for carbon tetrachloride. Comparison of the calculated values with those obtained experimentally by the "brightness" method	32
9	Shock temperature of carbon tetrachloride calculated using the constant $C_v$ model. Sensitivity of the calculated temperatures to the values used for $C_v$ and $(\partial p/\partial T)_v$	36
10	Shock temperature for carbon tetrachloride. Sensitivity of the calculated temperatures to the form of the Hugoniot	37
11	Shock temperature for nitromethane	41
12	Shock temperature for water. Comparison of the constant $C_v$ model with the Rice-Walsh constant $C_p$ model	43
13	Comparison of shock Hugoniot for water calculated from the "universal Hugoniot" with the experimental values measured by Rice and Walsh <sup>5</sup>	44
14	VLPP data for NF compounds and DTBP	54
15	Reaction coordinate diagram for the reaction: $C=C + N_2F_4 \rightleftharpoons F_2N - C - C - NF_2$	56

TABLES

Table

1	Shock properties of liquids	5
2	LVD gap sensitivity of 1,2-DP: Wall thickness studies	15
3	Effect of confinement on the LVD gap sensitivity	20
4	Correlation of sensitivity tests with reaction rates	21
5	Some thermodynamic properties and the LVD gap sensitivities of selected explosives	24
6	Comparison of shock temperatures for carbon tetrachloride calculated from Eq. (7) by trapezoidal evaluation of the integral and shock temperatures calculated by a Runge-Kutta integration of Eq. (6)	45
7	Input data for calculating shock temperatures	47 & 48
8	Sensitivity of the shock temperature of carbon tetrachloride to the values of $C_v$ and $(\partial p/\partial T)_v$	49
9	P-v Hugoniot for carbon tetrachloride calculated from $U_s = u_1 c_0 + u_2 u_p$	50

**BLANK PAGE**

GLOSSARY OF COMPOUNDS

<u>Code Name</u>	<u>Structure</u>	<u>Chemical Name</u>
2,3-BIB	$\text{CH}_3-\underset{\text{NF}}{\text{C}}-\text{C}-\underset{\text{NF}}{\text{C}}-\text{CH}_3$	2,3-bis(fluorimino)butane,
TBD	$(\text{CH}_3)_3\text{CNF}_2$	<i>t</i> -butyldifluoramino
2,3-DB-1, -2	$\text{CH}_3-\underset{\text{NF}_2}{\text{CH}}-\text{CH}-\text{CH}_3$	2,3-bis(difluoramino)butanes, diastereoisomers
1-DB	$\text{CH}_3\text{CH}_2\text{CH}_2\text{CH}_2\text{NF}_2$	1-difluoraminobutane
2-DB	$\text{CH}_3\text{CH}_2\text{CH}(\text{NF}_2)\text{CH}_3$	2-difluoraminobutane
DDP	$\begin{array}{c} \text{NF}_2 \\   \\ \text{CH}_3-\text{C}-\text{CN} \\   \\ \text{NF}_2 \end{array}$	2,2-bis(difluoramino)propionitrile
DIN	$\begin{array}{c} \text{NF}_2 \\   \\ \text{CH}_3-\text{C}-\text{CN} \\   \\ \text{CH}_3 \end{array}$	2-difluoramino-2-methylpropionitrile
DTBP	$(\text{CH}_3)_3\text{COOC}(\text{CH}_3)_3$	di- <i>t</i> -butyl peroxide
1,1-DP	$\begin{array}{c} \text{NF}_2 \\   \\ \text{CH}_3\text{CH}_2\text{CH} \\   \\ \text{NF}_2 \end{array}$	1,1-bis(difluoramino)propane
1,2-DP	$\text{CH}_3-\underset{\text{NF}_2}{\text{CH}}-\text{CH}_2-\text{NF}_2$	1,2-bis(difluoramino)propane
1,3-DP	$\text{F}_2\text{NCH}_2\text{CH}_2\text{CH}_2\text{NF}_2$	1,3-bis(difluoramino)propane
2,2-DP	$\text{CH}_3\text{C}(\text{NF}_2)_2\text{CH}_3$	2,2-bis(difluoramino)propane
FDB	$\begin{array}{c} \text{NF}_2 \quad \text{NF} \\   \quad \quad   \\ \text{CH}_3-\text{C}-\text{C}-\text{CH}_3 \\   \quad \quad   \\ \text{NF}_2 \quad \quad \text{NF} \end{array}$	2,2-bis(difluoramino)-2-fluorimino- butane
FIMB	$\begin{array}{c} \text{NF}_2 \quad \text{NF} \\   \quad \quad   \\ \text{H}_3\text{C}-\text{C}-\text{C}-\text{CH}_3 \\   \quad \quad   \\ \text{CH}_3 \quad \quad \text{NF}_2 \end{array}$	2-fluorimino-3-difluoramino-3- methylbutane
IBA	$\begin{array}{c} \text{NF}_2 \\   \\ \text{CH}_3-\text{C}-\text{CH}_2\text{NF}_2 \\   \\ \text{CH}_3 \end{array}$	1,2-bis(difluoramino)-2-methyl- propane

<u>Code Name</u>	<u>Structure</u>	<u>Chemical Name</u>
NFP	$\text{CH}_3-\underset{\text{NF}}{\text{C}}-\text{C}\equiv\text{N}$	N-fluoriminopropionitrile
2,2,3-TB	$\begin{array}{c} \text{NF}_2 \quad \text{NF}_2 \\   \quad   \\ \text{CH}_3-\text{C}-\text{CHCH}_3 \\   \\ \text{NF}_2 \end{array}$	2,2,3-tris(difluoramino)butane
TMEA	$\begin{array}{c} \text{NF}_2 \quad \text{NF}_2 \\   \quad   \\ \text{CH}_3-\text{C}-\text{CH}-\text{CH}_3 \\   \\ \text{CH}_3 \end{array}$	2,3-bis(difluoramino)-2-methylbutane (trimethylethylene adduct)
1,2,2-TP	$\begin{array}{c} \text{NF}_2 \\   \\ \text{CH}_3-\text{C}-\text{CH}_2\text{NF}_2 \\   \\ \text{NF}_2 \end{array}$	1,2,2-tris(difluoramino)propane

## I INTRODUCTION

Under the sponsorship of the Office of Naval Research, Stanford Research Institute is studying fundamental sensitivity properties of liquid high-energy materials in order to obtain basic knowledge on the ease of initiation and the characteristics of propagation, especially in relationship to chemical structure. In this work we have been primarily concerned with: (a) detonatability of the liquid phase, i.e., whether it will support a detonation wave, and the failure diameter for detonation; (b) the necessary conditions for initiating detonation and whether ease of initiation is related to structure; and (c) the mode of decomposition of the chemical structure and the relationship of the initial decomposition steps with the phenomena of (a) and (b).

In previous work on this contract,<sup>1</sup> these relationships have been studied with isomeric difluoramino propanes and butanes and we have now begun study on nitro compounds in the analogous isomeric propane series. Thus a direct comparison between the two high-energy groupings which are of most interest at present can be made, and basic knowledge can be obtained on the initiation and propagation properties of model liquid nitroaliphatic plasticizers.

This program consists of three primary tasks:

A. The detonation wave characteristics of the liquid phase

Difluoramino compounds are detonatable at low failure diameters and possess a high-velocity detonation rate of about 6 mm/ $\mu$ sec. However, they also have a more easily initiated low-velocity detonation region. The most recent work has emphasized study of low-velocity detonation (LVD) particularly aimed at characterizing this unusual phenomenon (Section II). Specifically, the objectives are to determine if the phenomenon is general under conditions of larger diameter and differing materials of confinement, to determine how easily LVD initiation occurs, and to relate the LVD to chemical decomposition mechanisms.

## B. Physics and chemistry of detonation

The ultimate objective of studies of the physics and chemistry of detonation (Section III) is to correlate transient detonation phenomena, such as shock initiation and failure behavior, with the mode of decomposition. This objective involves: (a) measurement of failure diameters; (b) study of events in the liquids as shocks of various magnitudes enter; and (c) measurements of reaction times at pressures and temperatures comparable to those encountered in initiating shocks. During the past six months, reaction time measurements made in shocked difluoramino compounds and calculation of the shock temperature have received considerable emphasis; these measurements are pertinent to failure diameter theory, dark waves, and high-temperature chemical kinetics in the liquid phase.

## C. The mechanism and kinetics of thermal decomposition in the gas phase

Section IV of this report comprises a study of the decomposition behavior of NF compounds and describes a relationship between detonation phenomena and chemical mechanisms. Most recently emphasis has been given to obtaining knowledge of the first few steps of decomposition under conditions of very-low-pressure pyrolysis (VLPP) and correlating these with the low-velocity and high-velocity detonation phenomena. In addition, the VLPP study provides knowledge of the initial bond-breaking reaction and bond energies of simple difluoramino groupings. The study is being extended to an isomeric series of dinitropropane compounds; during this period some initial data on mononitropropanes were obtained.

The Appendix to this report contains a list of papers, which document various phases of this program and are in the process of publication in the technical literature.

## References

1. Stanford Research Institute Project 4051, Technical Progress Report 66-2 (annual), "Sensitivity Fundamentals," March 1966, et seq.

## II LOW-VELOCITY DETONATION

(R. W. Woolfolk and H. R. Bredfeldt)

### A. Introduction

We have been studying low-velocity detonation (LVD) in the difluoramino compounds. Our efforts have concentrated on the sensitivity of these materials to LVD initiation. The gap sensitivity test has been the primary means of determining the important LVD initiation parameters. Using the difluoramino propanes and butanes and other appropriate model compounds we have determined the effect of confinement geometry, sonic velocity, wall thickness, and charge diameter on the apparent LVD gap sensitivity. We are now beginning to investigate the importance of physical and chemical properties of materials on LVD initiation. Our theoretical and experimental studies have shown that precursor cavitation does exist under gap test conditions. We have found agreement between what is predicted theoretically and what is found experimentally. The presence of precursor cavitation has previously been reported by the workers at the Bureau of Mines.<sup>1</sup>

Believing that cavitation may play a major role in LVD initiation and propagation, we derived a correlation between the heat of reaction ( $\Delta H_r$ ), the heat of vaporization ( $\Delta H_v$ ), and the LVD gap sensitivity. This correlation was remarkably good considering its simple nature.

The "universal Hugoniot" for liquids was improved by the addition of new data and the use of sonic velocities corrected to the experimental temperature. Because we feel further refinements are not justified by the imprecise nature of the data, this completes our efforts in this area.

We have shown that the use of 2-(2',4'-dinitrobenzyl)-pyridine (DNBP) to follow shock wave flow fields is not practical under our test conditions and further work in this area will not be continued.

## B. Theoretical Studies

### 1. Universal Hugoniot

Previous reports<sup>2,3</sup> have described an empirical method for estimating the Hugoniot of liquids. This equation was developed using the data of Rice and Walsh<sup>4</sup> with later addition of some data from Cook and Rogers.<sup>5</sup> A recent Russian publication<sup>6</sup> suggested the following representation

$$U_s = 1.2(c_o) + 1.7 u_p \quad (1)$$

where  $U_s$  is the shock velocity,  $c_o$  is the sonic velocity, and  $u_p$  the particle velocity. Our representation (Eq. 2) differed from Eq. (1) in a slight, but what appeared to be a statistically significant, manner.

$$U_s = 1.3_1 (c_o) + 1.6_1 u_p \quad (2)$$

Since both equations had used some of the same data we did not understand the difference. Therefore we undertook a review of the data. New results by Dick<sup>7</sup> of LASL were added and the data of Cook and Rogers were removed because they did not include their initial experimental temperature. We normalized the data with  $c_o$  corrected to the experimental temperature. Only those data below the transition point reported by Dick were used. The temperature correction for  $c_o$  was obtained from the literature or estimated by the methods outlined in Reid and Sherwood.<sup>8</sup> The corrected data appear in Table 1.

A least squares fit of this data (Fig. 1) is represented by Eq. (3)

$$U_s = 1.3_7 (c_o) + 1.6_2 u_p \quad (3)$$

The "universal Hugoniot" in the p-v plane appears in Fig. 2. The curve through the data was obtained using the Hugoniot relationship and Eq. (3). The scatter in the data was reduced by applying the temperature correction, but some scatter remains, reflecting the difficulties in obtaining very accurate experimental Hugoniot data on liquids. The

Table 1

## SHOCK PROPERTIES OF LIQUIDS

Compound	T °C	C <sub>0</sub> mm/μsec	ρ <sub>0</sub> g/cc	P kbar	U <sub>s</sub> mm/μsec	u <sub>p</sub> mm/μsec	v/v <sub>0</sub>
Benzene	12	1.379	.877	147	6.00	2.75	.541
	14	1.367	.885	75.3	4.79	1.78	.630
	14	1.367	.885	47.1	4.05	1.31	.676
	<sup>a</sup> 16	1.356	.883	52.4	4.10	1.45	.647
	18	1.345	.881	52.1	4.09	1.45	.646
	19	1.340	.890	110	5.52	2.26	.591
	19	1.340	.880	41.3	3.85	1.22	.684
	20	1.335	.879	29.8	3.47	.98	.719
	22	1.325	.877	47.6	4.05	1.34	.669
	22	1.325	.877	15.0	2.78	.61	.776
	24	1.313	.875	106	5.64	.21	.596
	24	1.313	.875	29.1	3.44	.97	.719
	27	1.298	.871	75.4	4.77	1.81	.620
	28	1.293	.870	99.5	5.28	2.17	.589
	28	1.293	.870	88.7	5.00	2.04	.591
	28	1.293	.870	25.8	3.31	.90	.730
	28	1.293	.870	18.9	2.96	.73	.753
	29	1.288	.869	67.4	4.52	1.72	.620
	29	1.288	.869	62.3	4.38	1.63	.627
	29	1.288	.869	17.4	2.72	.73	.730
	30	1.283	.868	124	5.71	2.50	.562
	<sup>a</sup> 32	1.273	.866	121	5.66	2.47	.564
	Carbon- disulfide	<sup>a</sup> 14	1.175	1.272	55.8	3.47	1.26
17		1.165	1.267	58.5	3.37	1.415	.580
18		1.161	1.266	61.9	3.51	1.39	.603
19		1.159	1.264	50.0	3.39	1.17	.655
20		1.155	1.263	36.5	3.09	.94	.697
22		1.149	1.260	56.4	3.47	1.29	.628

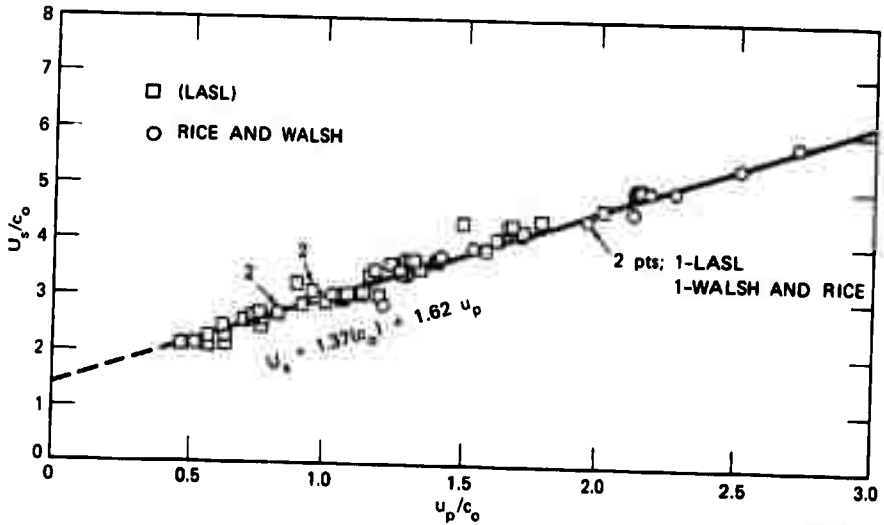
Table 1 (Cont'd)

Compound	T °C	C <sub>0</sub> mm/μsec	ρ <sub>0</sub> g/cc	P kbar	U <sub>B</sub> mm/μsec	u <sub>p</sub> mm/μsec	v/v <sub>0</sub>
Carbon- tetra- chloride	22	1.149	1.260	18.5	2.47	.59	.761
	24	1.143	1.257	35.7	3.06	.93	.696
	28	1.130	1.251	31.6	2.94	.86	.707
	28	1.130	1.251	22.9	2.59	.71	.727
	29	1.126	1.249	21.3	2.41	.71	.705
	32	1.116	1.245	53.6	3.43	1.26	.634
	14	.964	1.606	106	4.08	1.61	.604
	14	.964	1.606	66.7	3.46	1.20	.652
	18	.956	1.598	74.0	3.50	1.33	.621
	19	.948	1.596	153	4.71	2.04	.566
	19	.948	1.596	58.7	3.28	1.12	.658
	20	.945	1.594	42.3	2.95	.90	.694
	<sup>a</sup> 22	.943	1.591	73.9	3.51	1.325	.623
	22	.943	1.591	67.4	3.44	1.23	.643
	22	.943	1.591	21.3	2.32	.58	.752
	24	.936	1.586	148	4.66	2.00	.572
	24	.936	1.586	41.3	2.91	.90	.692
	27	.925	1.581	106	4.07	1.65	.596
	28	.921	1.579	140	4.52	1.96	.566
	28	.921	1.579	125	4.27	1.86	.565
	28	.921	1.579	36.4	2.79	.82	.702
	28	.921	1.579	26.6	2.47	.69	.722
	29	.919	1.577	95.1	3.86	1.57	.594
	29	.919	1.577	88.1	3.74	1.49	.601
	32	.910	1.571	24.7	2.27	1.69	.697
	32	.910	1.571	62.8	3.32	1.20	.637
	Acetone <sup>a</sup>	26	1.77	.7835	105.8	5.37	2.51
30		1.157	.7793	46.4	3.97	1.49	.624

Table 1 (Cont'd)

Compound	T °C	C <sub>0</sub> mm/μsec	ρ <sub>0</sub> g/cc	P kbar	U <sub>s</sub> mm/μsec	u <sub>p</sub> mm/μsec	v/v <sub>0</sub>
Ethyl ether <sup>a</sup>	21	.996	.7122	41.8	3.88	1.52	.610
	32	.936	.6995	96.1	5.40	2.55	.528
Ethanol <sup>a</sup>	21	1.158	.7893	47.3	4.03	1.487	.632
	26	1.140	.7844	110.4	5.63	2.50	.556
Methanol <sup>a</sup>	15	1.139	.7960	46.6	3.93	1.483	.625
	<sup>a</sup> 24	1.108	.7877	109.5	5.51	2.525	.542
Hexane <sup>a</sup>	19	1.086	.6599	41.5	4.02	1.517	.623
	<sup>a</sup> 32	1.031	.6487	95.7	5.54	2.59	.533

<sup>a</sup>Data from Rice and Walsh (Ref. 4).



TA-4081-436

FIGURE 1 NORMALIZED  $U_s - u_p$  PLOT

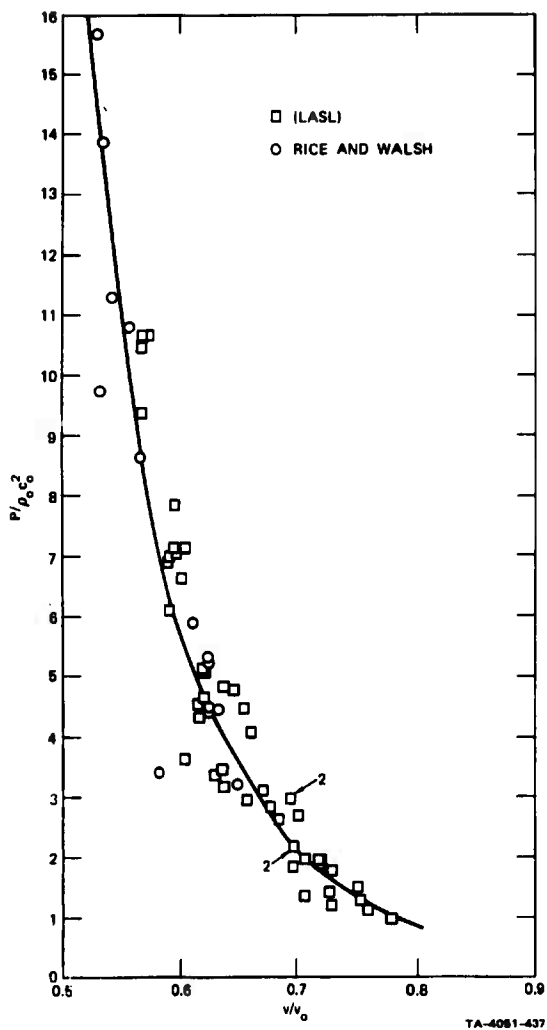


FIGURE 2 NORMALIZED  $p - v/v_0$  PLOT

Hugoniot for the difluoroamino propane and butane that appeared in the last report were calculated using Eq. (2). The difference between Eqs. (2) and (3) is not large enough to warrant a recalculation and will have very little effect on the shock temperature calculation presented by Shaw.<sup>2</sup> (See also Section III.) We feel that the present representation for a "universal Hugoniot" (Eq. 3) is adequate for estimation purposes and we will not devote further time to its development.

## 2. The Role of Cavitation in Liquid Sensitivity Testing

The term "cavitation" refers to the formation of liquid-vapor or liquid-gas interfaces, either at a liquid-solid boundary or in the interior of a liquid. In the former case, the resulting cavities are often relatively large, as that found behind a dense object dropped into a pool of water or around a ship's propeller. On the other hand, cavities formed in the interior of a liquid generally are small enough for their shape to be strongly influenced by surface tension: such cavities usually appear in the form of spherical or nearly spherical bubbles. Cavitation of this kind--sometimes called bulk cavitation because of the presence of a large number of bubbles at the same time--occurs when the pressure in a large volume of liquid is gradually reduced below the liquid vapor pressure or the saturation pressure of dissolved gases (effervescence); or when a tensile stress wave propagates through the liquid. Depending on whether the ambient pressure field leading to cavitation is semistatic or dynamic, the cavitation formation and growth process is governed by different parameters. A slowly varying ambient pressure field usually leads to the appearance of gas, or gas-vapor-mixture filled bubbles, while large magnitude tensile stress waves produce spalling in the liquid, which manifests the formation of nearly pure vapor bubbles. Pure vapor cavitation, unlike gas bubble cavitation, cannot be eliminated by degassing a liquid.

Pure vapor cavitation is of particular interest in liquid explosive sensitivity testing because large magnitude negative stress fields are generally associated with the event of shock impulses propagating through the test liquid. The negative stress fields are produced indirectly in the test liquid as a consequence of primary shock propagation.

The overall shock impulse consists of several pulses. First to enter the test liquid is, of course, the primary shock. This primary peaked compression wave is subsequently followed by secondary and higher order waves representing the first and higher order reflections of the various attenuator surfaces. Cavitation at the attenuator-liquid interface caused by rarefaction waves reflected from attenuator free surfaces has been observed in several experiments.<sup>2, 9, 10</sup>

As the main shock is transmitted to the liquid under test, it produces local high pressure regions in the liquid which in turn excite several vibrational modes of the container wall, similar to the familiar water-hammer phenomena.<sup>11</sup> It is assumed here that the stress levels set up in the wall do not exceed the elastic limit of the wall material. The wall stress waves in turn cause the liquid-solid boundary to oscillate and radiate pressure waves into the bulk of the liquid, giving rise to a feed back loop in the experimental system.

In terms of magnitude of the wall deflections, which determines the strength of the wall-radiated pressure waves in the liquid, the wall flexural waves and wall shear waves are of most importance. If the characteristic wall wave speed is higher than the speed of the primary shock in the liquid, the wall vibrations will propagate ahead of the primary shock, and cause precursor pressure wave disturbances. Positive and negative stress levels on the order of 1/10 kbar in the liquid can be produced by the wall precursor wave systems. These stress levels are sufficient to produce cavitation in most low viscosity liquids such as water.

There are basically 4 different sources of pure vapor cavitation in liquid explosive sensitivity testing. In addition to wall precursor cavitation,<sup>12</sup> and cavitation existing at the attenuator liquid interface, cavitation can be produced in weak containers due to radial, plastic wall deformation behind the primary shock<sup>13</sup> and also in the bulk of the liquid, as the primary, peaked shock wave is reflected off the free liquid surface cavitation behind the primary shock should start at the wall and then appear along the Mach lines toward the center of the container. Precursor cavitation may or may not start at the walls,

depending on the magnitude of the wall deflections, and is most likely to be observable near the center of the container where wave interaction gives rise to maximum stress levels. Both cavitation at the attenuator liquid-interface and near the free surface of the liquid should appear first through the central region of the container. Thus the location of the first appearance of cavitation may give a clue as to the type of negative stress wave.

Very little data are available for predicting the single pulse cavitation threshold stress levels. Experiments in the field of acoustic cavitation<sup>14</sup> indicate the cavitation threshold conditions depend on the size of the cavitation nuclei present in the liquid, on the pulse length,<sup>15</sup> on the liquid viscosity, and other factors.<sup>16</sup> Bull<sup>9</sup> found from single-pulse experiments in various liquids that the negative cavitation threshold stresses varied with viscosity raised to the 1/5 power. However, his results are somewhat in question since he did not determine the size of the cavitation nuclei present in his test liquids, and it is the latter parameter which is thought to have a major effect on the cavitation threshold.

The energy necessary for initiation of the exothermic decomposition process inside the vaporous cavity and/or in the surrounding liquid is provided by the bubble collapse process. Bubble collapse is brought about by either overexpansion of the bubble beyond the diameter in the equilibrium with the ambient pressure, or by a second compression pulse. Cavities collapsing with sufficient violence to reach spontaneous ignition conditions inside the bubble can constitute hot spots in the explosive liquid. In the vaporous cavity, the effect of vapor compression can be reduced by vapor condensation at the liquid-vapor interface. However, condensation produces a large amount of energy release which is difficult to dissipate in an environment undergoing shock compression. The amount of vapor that can be condensed therefore is limited by the energy losses to the ambient liquid. In general, the development of hot spots in a liquid explosive can have three possible consequences: the energy losses from a small, isolated hot spot to the liquid may be too large to sustain a reaction and the hot spot may disappear; the

hot spot may initiate slow deflagration burning in the liquid, which could account for low-velocity detonation if the hot spots are homogeneously distributed across the container cross section; or, under appropriate experimental conditions, the hot spot may initiate a high-velocity detonation.

In summary, two types of cavitation are of interest in shock sensitivity experiments: gas or gas-vapor filled bubbles and pure vaporous cavitation. While the above discussion dealt mostly with pure vaporous cavitation, the presence of gas-filled bubbles could greatly increase the shock impulse sensitivity characteristic of the liquid explosive. However, gas bubbles can be easily eliminated by degassing the liquid. Vaporous cavitation visually appears in the presence of peaked compression pulses such as those used in gap sensitivity testing. The occurrence of vaporous cavitation depends not only on the physical parameters of the liquid, such as viscosity, surface tension, etc., but also on the degree of purity of the liquids, the size of heterogeneous cavitation sites present, and the negative stress level in the liquid. Some of the effects of the physical liquid parameters on the sensitivity will be discussed in later sections. Vaporous cavitation can give rise to detonation initiation phenomena similar to the gas filled bubbles but, in addition, the observed existence of a cavitation front velocity is intriguing as a possible support for the cavitation hypothesis of LVD.

### C. Experimental Studies

#### 1. Cavitation and Shock Sensitivity Testing

As stated above, we have been investigating shock wave interaction in LVD gap sensitivity testing. Previous reports (2,3) have described some of these efforts. Recently we have obtained shadowgraphic pictures of cylindrical steel containers of nitromethane under typical gap test conditions. Plexiglas<sup>†</sup> windows 2.54 x 0.63 cm allowed visual pictures to be taken of the liquid under shock stress conditions. The tubes were 2.54 cm in diameter and 10.4 cm in length with wall thickness of 0.63 cm. The results of these studies are shown in Fig. 3, where eight

---

<sup>†</sup>Trademark, Rohm & Haas Co.

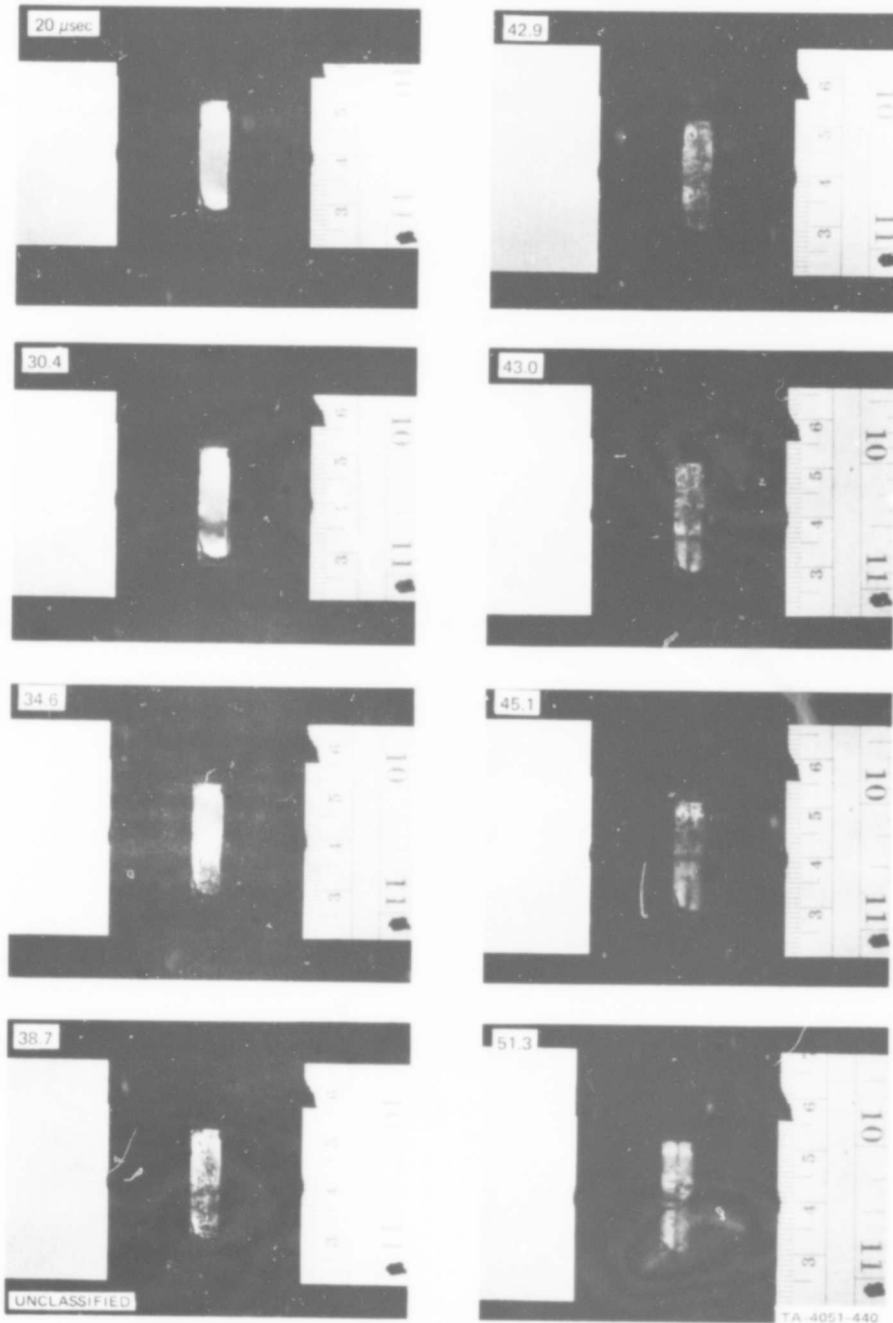


FIGURE 3 CAVITATION IN SHOCKED NITROMETHANE (U)

selected frames from a twenty-five-frame sequence are listed. The initial shock was produced by a 100-gram tetryl booster and attenuated by 2.54 cm of Plexiglas. The window was situated midway up the tube. The framing rate was 2.08  $\mu\text{sec}/\text{frame}$  and the number on each frame indicates the number of  $\mu\text{sec}$  from initiation. The shock wave arrives at the Plexiglas-tube interface at 19  $\mu\text{sec}$ . Crossed precursor waves are seen in the 30.4  $\mu\text{sec}$  frame. (The photographs reproduced here are half-tone prints which represent a reduction from a 1/128 gray scale for the negative to 1/12 for these prints. Therefore some of the details seen in the negatives are lost in the reproduction.) Two frames later (34.6  $\mu\text{sec}$ ) bubbles are clearly visible following the passage of the precursor waves (seen at top of window). The primary liquid shock arrives in the fifth frame (42.9  $\mu\text{sec}$ ) and the bubbles are compressed by its passage; however, not all of the bubbles appear to be compressed by the liquid shock. In the later frames the Plexiglas windows show signs of cracking.

The precursor wave has an average velocity of about 2.5  $\text{mm}/\mu\text{sec}$ ; however one would expect this velocity to be nearer that of the steel wall sonic velocity of 5.0  $\text{mm}/\mu\text{sec}$ . The bubble front velocity varies from 2.0 to 3.5  $\text{mm}/\mu\text{sec}$  and appears to be increasing with time. The liquid shock velocity, as expected, decreases from 2.0 to  $\sim 1.0$   $\text{mm}/\mu\text{sec}$  during its passage across the viewing port. These preliminary results are in qualitative agreement with that outlined above concerning cavitation in gap test experiments. More quantitative work is needed, however, before a detailed picture of cavitation can be obtained and compared to theoretical studies. We are planning to refine our techniques to include Schlieren photography which is more sensitive to the density gradient in a stress wave.

## 2. Effects of Confinement on LVD Gap Sensitivity

In the last report<sup>2</sup> we presented preliminary data on the effects of wall thickness on the LVD gap sensitivity. The analyzed results (Table 2) show that the apparent LVD gap sensitivity of 1,2-DP increases with decreasing wall thickness. However, there does appear to be a

Table 2

LVD GAP SENSITIVITY OF 1,2-DP: WALL THICKNESS STUDIES  
(STEEL TUBES 1.27 cm i.d., 10-cm LENGTH)

Wall (cm)	LVD Gap (cm Plexiglas)	LVD Transit Velocity (mm/ $\mu$ sec)
0.63	30 < - > 40.6	2.3 <sub>1</sub>
0.23	61 < - > 122	2.4 <sub>2</sub>
0.12	91.5 < - > 107 LVD unstable	~ 2.4

minimum thickness below which the LVD becomes unstable and does not propagate. These facts are further evidence of the coupling of the LVD reaction wave with the confinement walls. It appears that if the walls become too thin they cannot support a stable LVD wave. Lateral wall movement may occur so rapidly that the reactions are quenched before the energy is fully released. Figure 4 depicts four selected frames from a high speed framing camera sequence of an LVD gap sensitivity test using 1,2-DP. The tube wall thickness is 0.12 cm. Unstable LVD is seen to begin in the 535  $\mu$ sec frame as the tube begins to swell. By 552  $\mu$ sec the reaction has proceeded unstably to the top of the tube and also has split the tube walls. In the thicker-walled tests the reaction always began at the bottom and proceeded normally to the top of the tube. The initiation, however, was delayed on the order of 100  $\mu$ sec after the initial donor shock wave had reached the tube-attenuator interface. This delay seems to be characteristic of the LVD reaction in 1,2-DP when large gaps (> 30 cm) are used.

We have completed some of the preliminary studies on the effect of charge diameter on the LVD gap sensitivity. Using IBA as a model compound, we determined the LVD gap sensitivity in 2.54 and 1.27 cm diameter steel tubes (wall thickness 0.22 cm). The LVD gap sensitivity appears to increase with increasing charge diameter. However these results may only reflect the change in strength of the wall as the diameter is increased. We are planning to test this idea by a set of

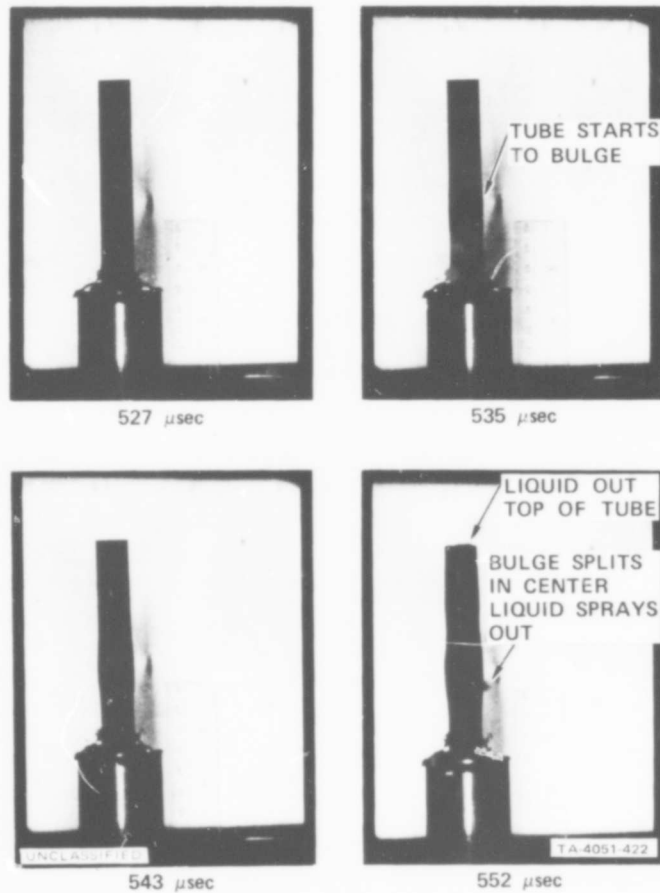


FIGURE 4 UNSTABLE LVD IN 1,2-DP (0.12 cm tubes) (U)

experiments in which the ratio of the inside diameter (D) to wall thickness (t) remains constant. We will do this for two values of D/t. These results will be discussed in the next report.

### 3. Study of Tracer Dye Technique

In conjunction with our studies of the shock wave interaction occurring in gap sensitivity testing, we investigated the possibility of using a tracer dye technique to follow the flow field behind these shock interactions. This technique was developed by Popovich and Hummel<sup>17</sup> to follow developing boundary layers. The tracer material, 2-(2',4'-dinitrobenzyl)-pyridine (DNBP), is colorless until it is activated to a colored tautomeric form by uv light. Since the colored form will persist for several milliseconds, this material can be used as a tracer in a flow field. We had planned to flash-photolyze a thin-colored line before the arrival of the weak shock waves and then follow the shock flow field by high speed photography. The colorless material strongly absorbs only about 3000 Å, but nitro and nitrate groups common to most liquid explosives strongly absorb in this region (See Fig. 5). Therefore, this technique would require the use of a non-explosive liquid. The difluoramino compound could be used since they do not begin to strongly absorb until 2000 Å, but they may not be compatible with the dye material. In addition, as Fig. 6 shows, window material would be limited to uv transparent material like Vycor.<sup>†</sup> Plexiglas absorbs too strongly in the 3000 Å region to be useful. The colored form of DNBP (line 4, Fig. 6) has its absorption centered about 6000 Å so it could be photographed.

Using glass material for windows does present some difficult problems. The glass fracture rate under this condition is very high (5 mm/μsec) and this fracturing would likely interfere with subsequent pictures. The window material requirement presents a formidable barrier to the development of DNBP as a tracer dye for shock experiments with explosive liquids. On this basis we decided to abandon any further development of this technique.

---

<sup>†</sup>Corning Glass Works.

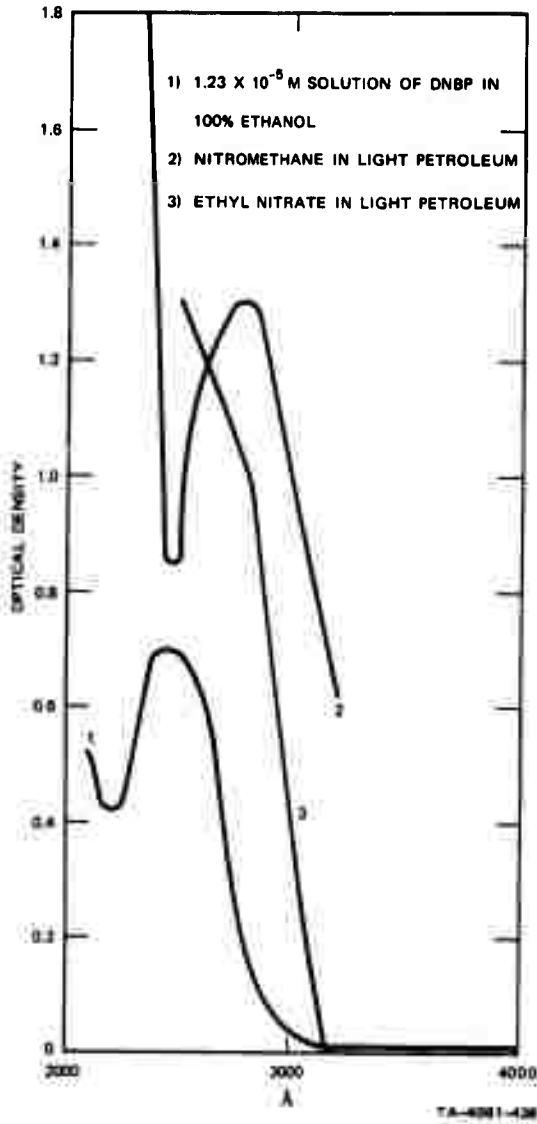


FIGURE 5 ABSORPTION SPECTRA OF THREE COMPOUNDS

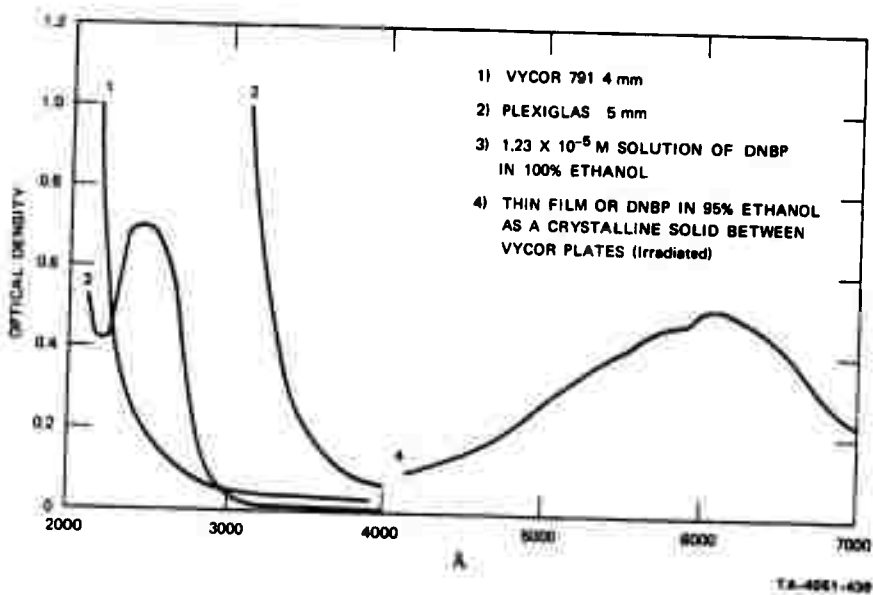


FIGURE 6 ABSORPTION SPECTRA OF WINDOW MATERIAL AND DNBP (Colored and Colorless)

#### D. Discussion

Our studies of LVD sensitivity in the difluoramino compounds have been guided by an attempt to discover the determining factors. Using the gap sensitivity test we have measured the effect of confinement on LVD sensitivity. These effects are summarized in Table 3.

Table 3  
EFFECT OF CONFINEMENT ON THE LVD GAP SENSITIVITY  
OF 1,2-DP

<u>Confinement Parameter</u>	<u>Effect</u>
Confinement geometry <sup>18</sup>	Increased sensitivity in cylindrical geometry.
Sonic Velocity <sup>18</sup>	Increased sensitivity with increased sonic velocity.
Wall thickness <sup>3</sup>	Increased sensitivity with decreased wall thickness (unstable in very thin walls)

It should be understood that these confinement effects may not generalize to all LVD-sustaining liquids, but we hope they can act as a useful guide to a probable mechanism. They support the proposition that in LVD there is a coupling of the explosive and its confinement. If this coupling is accomplished by precursor waves, then increasing the ratio of the wall sonic velocity to that of the liquid would magnify the effects of these waves. Decreasing the wall thickness (strength) also would act to magnify these effects. This is of course what is found experimentally. In cylindrical geometry there would be a stronger focusing effect on the precursor waves than in rectangular confinement. We have noted an increase in the LVD gap sensitivity in cylindrical geometry. The charge diameter studies are not yet complete so we will refrain from comment on their meaning at this time.

We have also studied the effects of chemical properties on LVD gap sensitivity. By comparing results obtained for various difluoramino isomers, we were able to show that compounds with the fastest low pressure reaction rate were the most sensitive to LVD.<sup>†</sup> In addition, we compared these results with other sensitivity tests. These comparisons (Table 4) show that there appears to exist a correlation between the gas phase reaction rate and the LVD, drop weight, and spark sensitivity. One conclusion that can be drawn from this correlation is that the reactions that lead to positive results in these tests are similar. The reaction of importance under these conditions is the scission of the C-N bond. This reaction is favored at low pressure and lower temperatures.

Table 4  
CORRELATION OF SENSITIVITY TESTS WITH REACTION RATES

Gas-Phase Reaction Rate	Sensitivity Test			Reaction Time HVD Gap
	LVD Gap	Drop Weight	Spark	
2,2-DP ↑ <sup>a</sup>	2,2-DP ↑	2,2-DP ↑	2,2-DP ↑	2,2-DP ↓ <sup>b</sup>
1,2-DP ↑	1,2-DP ↑	1,2-DP ↑	1,2-DP ↑	1,2-DP ↓
1,3-DP ↑	-- ↑	1,3-DP ↑	-- ↑	-- ↓

a ↑ = increasing sensitivity or reactivity

b ↓ = increasing reactivity.

On the other hand the high velocity detonation (HVD) reaction time correlates very well with the rate of elimination of hydrogen fluoride (HF). This reaction is favored under the conditions of high pressure and temperature that prevail in HVD.<sup>3</sup>

If the initiation of the LVD reaction is a low pressure-lower temperature phenomenon, what are the conditions that can provide this environment? In Section B-2 we discussed some of the parameters that

<sup>†</sup>The chemical kinetic data were obtained by D. S. Ross as a part of our overall studies of sensitivity fundamentals. See refs. 2 and 3 and Section IV for the details of these studies.

lead to cavitation. Precursor waves can lead to cavitation ahead of the primary liquid shock. The interaction between the liquid shock and cavitation could lead to initiation of LVD. However, we have noted in many LVD tests that there are long delays between the initial shock arrival and initiation of LVD. Therefore the situation is more complicated than this simple explanation would indicate.

If, however, cavitation is an important part of LVD then certain physical characteristics of the explosive should be the determining factors of LVD initiation. These factors include the heat release ( $\Delta H_r$ ), the heat vaporization ( $\Delta H_v$ ), the surface tension, the heat capacity, the sonic velocity, the viscosity, the gas solubility, and the chemical reaction kinetics. It appears that two of the more important parameters in LVD would be the heat of reaction and the heat of vaporization.  $\Delta H_r$  would supply the energy to drive the LVD wave and  $\Delta H_v$  would remove energy in the cavitation process. Table 5 lists several compounds for which we have calculated the heat of reaction based on the assumption of simple reaction products. The values of  $\Delta H_v$  in Table 5 were obtained from the literature or were calculated from the vapor pressure curves. We have also included the LVD gap sensitivities of these selected compounds.

Figure 7 is a plot of  $\Delta H_r/\Delta H_v$  as a function of the LVD gap sensitivity for the compounds in Table 5. We have included the two dinitropropane isomers as we are planning to obtain their LVD gap sensitivity. The correlation between  $\Delta H_r/\Delta H_v$  and the LVD gap sensitivity is very good considering this simple approach. This would further indicate that perhaps these physical chemical factors are the dominant ones in LVD. However, as we have stated above the reaction rate also plays an important role in LVD initiation. We have included nitroglycerine in Table 5 but not in Fig. 7 because we do not have a value for its LVD gap sensitivity. But we do know that its LVD sensitivity value is very large which would be indicated by the rather high value for  $\Delta H_r/\Delta H_v$ .

The purpose of correlation is to predict values for new materials. So we have estimated the LVD gap sensitivity of the dinitropropanes by calculating their  $\Delta H_r/\Delta H_v$ . Based on this estimation we would conclude

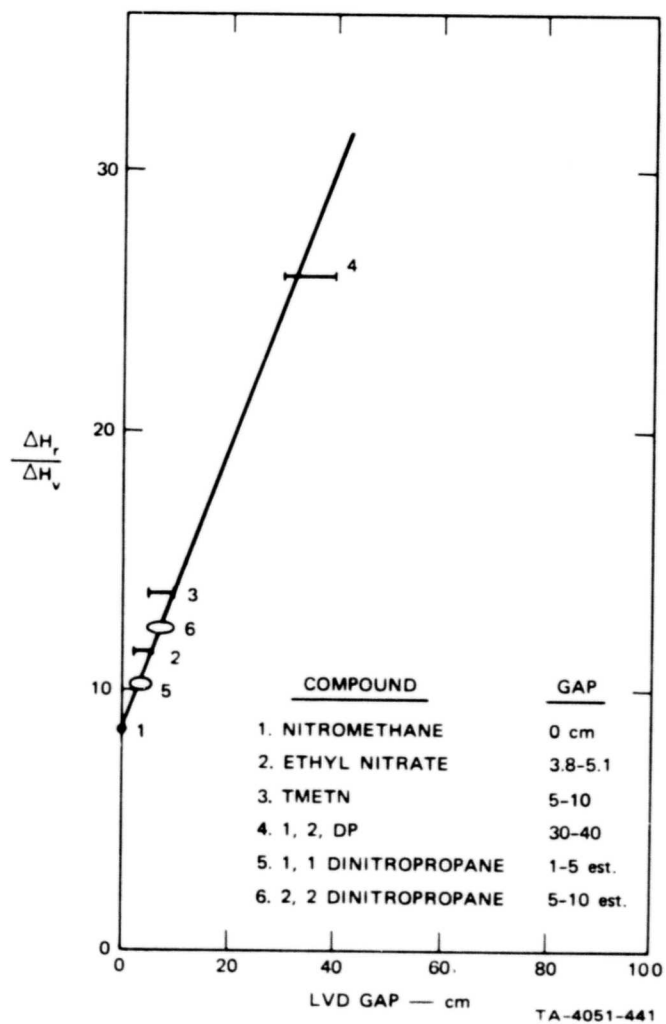


FIGURE 7 THERMODYNAMIC RATIO  $\Delta H_r/\Delta H_v$  VERSUS LVD GAP SENSITIVITY

Table 5

## SOME THERMODYNAMIC PROPERTIES AND THE LVD GAP SENSITIVITIES OF SELECTED EXPLOSIVES

Compound	Heat of Formation $\Delta H_f$	Heat of Vaporization $\Delta H_v$	Heat of Reaction $\Delta H_r$	LVD Gap Sensitivity <sup>a</sup>
	Kcal/mole	Kcal/mole	Kcal/mole	cm Plexiglas
Nitromethane	-27.03	9.09	-69.38	0
Ethyl Nitrate	-44.3	8.7	-100.2	3.8-5.1
TMETN	-105.8	20.7	-273.2	5-10
1,2-DP	-48.0	7.9	-205	30-40
1,1-Dinitropropane	-40.78	14.9	-152.04	1-5 Est. <sup>b</sup>
2,2-Dinitropropane	-44.87	12.0	-147.95	5-10 Est. <sup>b</sup>
Nitroglycerine	-90.75	19.17	-1214.5	very large

<sup>a</sup>Data obtained using either camera or probes as detectors.

<sup>b</sup>Values estimated from Fig. 7.

that these are not too sensitive. In fact, the 1,1-isomer may not show any LVD at all. We are planning to test them for LVD as soon as possible to see if we have made a correct estimate. It should be emphasized again that the parameter  $\Delta H_r/\Delta H_v$  is not the only one that may be important. In fact the chemical reaction kinetics should be taken into account. Nitromethane, which does not undergo LVD, has several of these factors against it. Its heat of reaction is low. Although its  $\Delta H_v$  is reasonable, its reaction kinetics are known to be very slow.

We hope in the future to develop a parameter that include many other factors of importance in LVD initiation. In this way one may be able to calculate, a priori, the LVD gap sensitivity of a new material from knowledge of its physical and chemical properties.

E. Future Work

We will continue our efforts to determine the important parameters in LVD gap sensitivity. From these studies we hope to derive more information about low-velocity detonation in general as well as LVD gap sensitivity in particular. During the next period we will continue theoretical studies of cavitation effects as well as experimental programs to complement these studies.

We will continue our efforts to obtain charge diameter effects on LVD gap sensitivity. In addition, we will study the effects of charge length on LVD sensitivity. The materials are now on hand for these studies.

Some effort will be expended in LVD studies of the dinitropropanes. We are particularly intrigued to discover if our prediction of their LVD gap sensitivities are correct.

We will also attempt to further develop correlation parameters for LVD gap sensitivity. In particular, we would like to include reaction kinetics and attempt to discover how other parameters correlate with LVD gap sensitivity; the ultimate aim of such studies being the prediction a priori of the sensitivity of new materials.

## References

1. R. W. Watson et al., "Detonations in Liquid Explosive--The Low-Velocity Regime," Proceedings Fourth Detonation Symposium, 1965, p. 117.
2. Stanford Research Institute Project 4051, Technical Progress Report 68-1 (Semiannual), "Sensitivity Fundamentals," April 15, 1969.
3. Stanford Research Institute Project 4051, Technical Progress Report 68-2 (Semiannual), "Sensitivity Fundamentals," September 15, 1968.
4. J. Walsh and M. Rice, *J. Chem. Phys.* 26, 815 (1957).
5. M. A. Cook and L. A. Rogers, *J. Appl. Phys.* 34, 2330 (1963).
6. I. M. Voskoboinikov, A. N. Afanasenkov, and V. M. Bogomolov, *FGV (Phys. of Expl. and Combustion)* No. 4, 585 (1967).
7. Richard D. Dick, "Shock Wave Compression of Benzene, Carbon Disulfide, Carbon Tetrachloride, and Liquid Nitrogen," Los Alamos Scientific Laboratories Project No. 3915, April, 1968, under AEC Contract No. W-7405 Eng. 36.
8. Robert C. Reid and Thomas K. Sherwood, *The Properties of Gases and Liquids*, McGraw-Hill Book Company, Inc., New York, 1958.
9. T. H. Bull, *Phil. Mag.* 1, No. 2, 153, February (1956).
10. F. L. Gibson, R. W. Watson, J. E. Hay, C. R. Summers, J. Ribovich, and F. H. Scott, Quarterly Report, Explosive Research Center, Bureau of Mines, Pittsburgh, Pennsylvania, January 1 to March 31, 1966.
11. R. Skalak, *Trans. ASME*, 78, 105 (1956).
12. A. B. Amster, D. M. McEachern, Jr., and Z. Pressman, "Detonation of Nitromethanes-Tetranitromethane Mixtures: Low and High Velocity Waves," Proceedings Fourth Detonation Symposium, 1965, p. 126.
13. F. C. Gibson, R. W. Watson, J. E. Hay, C. R. Summers, and F. H. Scott, Semiannual Report No. 3916, Explosive Research Center, Bureau of Mines, Pittsburgh, Pennsylvania, August 1 to January 31, 1964.
14. W. P. Mason, "Physical Acoustics, Principles and Methods," Vol. I, Part B, Academic Press, 1957.
15. D. Lieberman, *Phys. Fluids* 2, 466 (1959).

16. G. Kurtze, Nachr. Akad. Wiss. Göttingen, Math-Physik, Vol. IIA, Jan. 1 (1958).
17. A. T. Popovich and R. L. Hummel, Chem. Eng. Sci 22, 21 (1967).

**BLANK PAGE**

### III PHYSICS AND CHEMISTRY OF DETONATION

(M. Cowperthwaite and R. Shaw)

#### A. Introduction

This program is concerned with the transient detonation phenomena, shock initiation and failure. During the present reporting period we have concentrated on shock initiation. We have devoted most effort to solving one of the major problems in shock initiation--calculation of the shock temperature. Calculation of shock temperature is important in shock-initiation studies of liquid explosives because pressure-volume-temperature (p-v-T) equations of state of liquids in the kilobar region are not known. Use of the Walsh-Christian method<sup>1</sup> developed for metals is obviously limited by the assumptions upon which it is based. The assumption of constant specific heat at constant volume  $C_v$  is not valid for molecular liquids with internal degrees of freedom, neither is the assumption that numerical differences between  $C_v$  and specific heat at constant pressure  $C_p$  can be neglected for calculational purposes. It is necessary to account for those differences between liquids and solids to make the Walsh-Christian method more applicable to liquids. The present work provides a new method of calculating shock temperatures. It is based on a variational analysis which shows that calculated shock temperature is much more sensitive to changes in  $C_v$  than to changes in  $(\partial p / \partial T)_v$ . Shock temperatures for various liquids were calculated with both constant and variable  $C_v$  and those for carbon tetrachloride were compared with brightness temperatures measured by other workers.<sup>2,3</sup>

#### B. The Walsh-Christian Method of Calculating Shock Temperature

Cowperthwaite<sup>4</sup> has discussed the significance of two equations of state, the Walsh-Christian method (constant  $C_v$ ) used for metals<sup>1</sup> and the Rice-Walsh method (constant  $C_p$ ) used for water.<sup>5</sup> For the present work the Walsh-Christian method was preferred because it required less high pressure data.

Briefly, the basis of the method is as follows. From the Rankine-Hugoniot relations,

$$de = 1/2 (p_0 - p)dv + 1/2 (v_0 - v) dp \quad (1)$$

where  $e$  is the internal energy,  $p_0$  is the initial pressure (assumed to be negligible compared to the pressure at  $p$ ), and  $v_0$  is the initial volume.

$$de = 1/2 pdv + 1/2 (v_0 - v) dp \quad (2)$$

Further,

$$de = (\partial e / \partial T)_v dT + (\partial e / \partial v)_T dv \quad (3)$$

where  $T$  is the temperature. Substituting  $C_v$ , the heat capacity at constant volume for  $(\partial e / \partial T)_v$ , and  $[T(\partial p / \partial T)_v - p]$  for  $(\partial e / \partial v)_T$  in Eq. (3),

$$de = C_v dT + [T(\partial p / \partial T)_v - p] dv \quad (4)$$

Combining Eqs. (2) and (4),

$$C_v dT + T(\partial p / \partial T)_v dv = 1/2 pdv + 1/2 (v_0 - v) dp \quad (5)$$

dividing throughout by  $C_v dv$ , we obtain the differential equation along the Hugoniot

$$\frac{dT}{dv} + \frac{T(\partial p / \partial T)_v}{C_v} = \frac{1}{2C_v} [p + (v_0 - v) \frac{dp}{dv}] \quad (6)$$

Walsh and Christian showed that if  $(\partial p / \partial T)_v$  and  $C_v$  are constant Eq. (6) can be solved explicitly to give

$$T = T_0 e^{b(v_0 - v)} + \frac{e^{-bv}}{2C_v} \int_{v_0}^v e^{bv} F(v) dv \quad (7)$$

where  $b = (\partial p / \partial T)_v / C_v$  and  $F(v) = p + (v_0 - v)(dp/dv)$ .

A BASIC computer program was written by B. Y. Lew of SRI to calculate shock temperatures using Eq. (7). In the program the integral was evaluated by a trapezoidal approximation. The program was checked as follows. Walsh and Christian's input data for  $b$ ,  $C_v$  and  $F(v)$  for copper were used and excellent agreement was obtained with their shock temperatures. In addition, C. L. Mader of Los Alamos Scientific Laboratory kindly used our input data for nitromethane with his program and obtained agreement with our results.

Another way of calculating the shock temperature is to integrate the differential Eq. (6) using a Runge-Kutta technique. This is a more generally useful method because any function of  $C_v$  and  $(\partial p/\partial T)_v$  can be used. Of course, if constant values of  $C_v$  and  $(\partial p/\partial T)_v$  are used, then the shock temperatures calculated by the Runge-Kutta integration of Eq. (6) will be the same as those calculated by the trapezoidal evaluation of the integral in Eq. (7). This agreement was confirmed by the calculations for carbon tetrachloride shown in Table 6. The input data is in Table 7. The  $p$ - $v$  Hugoniot from which  $F(v)$  is derived is obtained by using the Rankine-Hugoniot relations to transform the universal liquid Hugoniot

$$U_s = u_1 c_0 + u_2 u_p \quad (8)$$

where  $U_s$  is the shock velocity,  $u_p$  is the particle velocity,  $c_0$  is the sound velocity at ambient, and  $u_1$  and  $u_2$  are constants.

In Fig. 8 the shock temperature for carbon tetrachloride calculated using constant  $C_v$  and  $(\partial p/\partial T)_v$  is compared with the "brightness" temperatures, previously measured by Voskoboinikov and Bogomolov<sup>2</sup> and by Ramsay.<sup>3</sup>

Clearly, the experimental and calculated results are in poor agreement. We consider it likely that the calculated values are "too high" or, in other words, the model for the calculated temperatures is too simple.

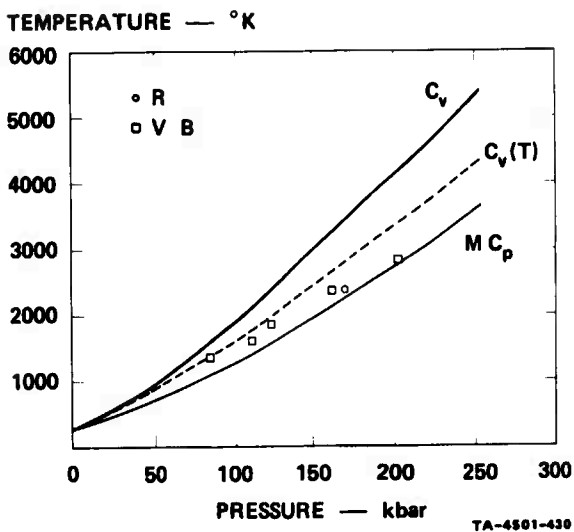


FIGURE 8 SHOCK TEMPERATURE FOR CARBON TETRACHLORIDE. Comparison of the calculated values with those obtained experimentally by the "brightness" method. The line  $C_v$  was calculated in the present work using constant  $C_v$ . The line  $M C_p$  was calculated by Mader (Ref. 3) using constant  $C_v$  but using  $C_p$  for the value of  $C_v$ . The dashed line  $C_v(T)$  was calculated in the present work using  $C_v$  as a function of temperature. The input data for the calculation are in Table 2.

C. Variational Analysis of the Walsh-Christian Method (Sensitivity of the Calculated Temperatures to the Values Chosen for  $(\partial p/\partial T)_v$  and  $C_v$ )

Of the three variables  $(\partial p/\partial T)_v$ ,  $C_v$ , and  $F(v)$  in the differential Eq. (6),  $F(v)$  is probably the best established. It may be assumed to be known. (It will later be shown empirically that the calculated temperature as a function of shock pressure is almost unaffected by using different forms for  $F(v)$ .)

Concerning  $(\partial p/\partial T)_v$  and  $C_v$ , consider integration between  $v_0$  and  $v_1$ . At  $v_1$ , let  $T_H$  be the temperature on the Hugoniot and let  $T_s$  be the temperature on the isentrope, given by  $T_s = T_0 \exp b(v_0 - v_1)$ . Consider the shock temperature at  $v_1$  to be a function of  $b$  and  $C_v$ , then from Eq. (7)

$$T_H(v_1, b, C_v) = T_s + \frac{e^{-bv_1}}{2C_v} \int_{v_0}^{v_1} e^{bv} F(v) dv \quad (9)$$

$$= T_s + \frac{1}{2C_v} \int_{v_0}^{v_1} e^{b(v-v_1)} F(v) dv \quad (10)$$

The slope of the  $T_H$  versus  $(\partial p/\partial T)_v$  curve is given by

$$\frac{\partial T_H}{\partial (\partial p/\partial T)_v} = T_s (v_0 - v_1) \left[ \frac{\partial b}{\partial (\partial p/\partial T)_v} \right] + \frac{1}{2C_v} \int_{v_0}^{v_1} (v-v_1) \left[ \frac{\partial b}{\partial (\partial p/\partial T)_v} \right] e^{b(v-v_1)} F(v) dv \quad (11)$$

Now  $b = (\partial p/\partial T)_v / C_v$  . . .  $\partial b/\partial (\partial p/\partial T)_v = 1/C_v$

$$\text{and } \frac{\partial T_H}{\partial (\partial p/\partial T)_v} = \frac{T_s (v_0 - v_1)}{C_v} + \frac{I}{2C_v^2} \quad (12)$$

$$\text{where } I = \int_{v_0}^{v_1} (v-v_1) e^{b(v-v_1)} F(v) dv$$

The RHS of Eq. (12) is positive, so increasing  $(\partial p/\partial T)_v$  will increase  $T_H$ . Similarly, the slope of the  $T_H$  versus  $C_v$  wave is given by

$$\frac{\partial T_H}{\partial C_v} = \left[ T_s (v_o - v_1) \frac{\partial b}{\partial C_v} \right] + \frac{1}{C_v} \int_{v_o}^{v_1} (v - v_1) \frac{\partial b}{\partial C_v} e^{b(v-v_1)} F(v) dv - \frac{1}{2C_v^2} \int_{v_o}^{v_1} e^{b(v-v_1)} F'(v) dv \quad (13)$$

Now  $b = (\partial p/\partial T)_v / C_v$  . .  $\partial b/\partial C_v = - (\partial p/\partial T)_v / C_v^2 = - b/C_v$

$$\begin{aligned} \therefore \partial T_H / \partial C_v &= -b \left[ \frac{T_s (v_o - v_1)}{C_v} + \frac{1}{2C_v^2} \right] - \left[ \frac{T_H - T_s}{C_v} \right] \\ &= - \left[ b \frac{\partial T_H}{\partial (\partial p/\partial T)_v} + \frac{(T_H - T_s)}{C_v} \right] \end{aligned} \quad (14)$$

The RHS of Eq. (14) is negative so that decreasing  $C_v$  results in an increase in  $T$ .

Let  $R = (\partial T_H / \partial C_v) / (\partial T_H / \partial (\partial p/\partial T)_v)$

$$\begin{aligned} \text{Then } R &= - \left[ \frac{\left( b \frac{\partial T_H}{\partial (\partial p/\partial T)_v} \right) + \left( \frac{T_H - T_s}{C_v} \right)}{\frac{\partial T_H}{\partial (\partial p/\partial T)_v}} \right] \\ &= - \left( b + \frac{T_H - T_s}{C_v (\partial T_H / \partial (\partial p/\partial T)_v)} \right) \\ &= - \left( b + \frac{T_H - T_s}{T_s (v_o - v_1) + v(1/2C_v)} \right) \end{aligned} \quad (15)$$

For a 10% increase in  $(\partial p/\partial T)_v$ , i.e.  $\Delta(\partial p/\partial T)_v = .1(\partial p/\partial T)_v$  and a 10% decrease in  $C_v$ , i.e.  $\Delta C_v = -.1 C_v$ , neglecting second and higher derivatives,

$$\frac{\Delta T(C_v)}{\Delta T(\partial p/\partial T)_v} = 1 + \frac{T_H - T_S}{b(T_S(v_0 - v_1) + (I/2C_v))} \quad (16)$$

As  $T_H$  is always greater than  $T_S$ , the shock temperature is more sensitive to  $C_v$  than to  $(\partial p/\partial T)_v$ . Equations (15) and (16) have been evaluated for carbon tetrachloride up to 250 kbar. The results in Table 8 show that, as the pressure increases up the Hugoniot,  $C_v$  becomes increasingly more important than  $(\partial p/\partial T)_v$ .

The above conclusions were confirmed empirically as shown by Fig. 9 and the last column of Table 8.

To test the effect of changing the p-v Hugoniot, the shock temperature was calculated for four different "universal" Hugoniots for carbon tetrachloride, namely

$$U_s = 1.2c_o + 1.7u_p \text{ (ref. 2)}, U_s = 1.25c_o + 1.7u_p \text{ (this work, arbitrary variation from 1.2 to 1.25)}, U_s = 1.199c_o + 1.672u_p \text{ (ref. 7)}, \text{ and } U_s = 1.31c_o + 1.61u_p \text{ (ref. 8)}.$$

The last Hugoniot had previously been suggested<sup>8</sup> as a better "universal" fit for liquids. The results in Fig. 10 show that the temperature as a function of shock pressure is little changed, although Table 9 shows that the p-v Hugoniots are significantly different.

#### D. Effect of Increasing Pressure and Temperature on $(\partial p/\partial T)_v$ and $C_v$

For carbon tetrachloride at atmospheric pressure around room temperature  $(\partial p/\partial T)_v$  increases with temperature.<sup>9</sup> But from Bridgman's work<sup>10</sup> on the p-v-T relation of liquids at high pressures,  $(\partial p/\partial T)_v$  decreases with increasing temperature at constant volume. Bridgman made a detailed investigation of the previously advanced hypothesis that  $(\partial p/\partial T)_v$  is a function of volume only. Although the relation

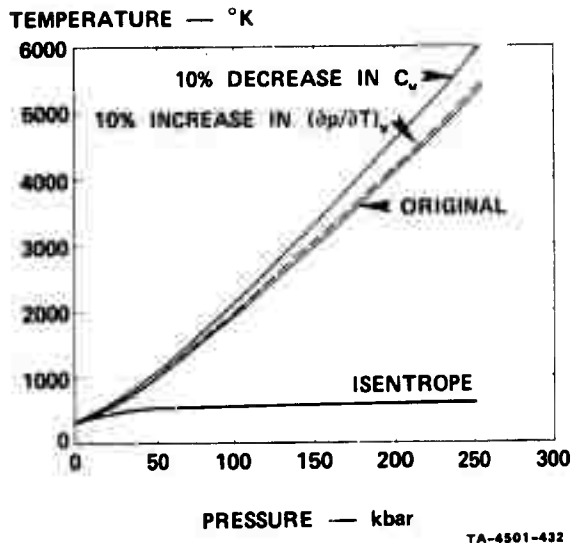


FIGURE 9 SHOCK TEMPERATURE OF CARBON TETRACHLORIDE CALCULATED USING THE CONSTANT  $C_v$  MODEL. Sensitivity of the calculated temperatures to the values used for  $C_v$  and  $(\partial p/\partial T)_v$ . The input data are in Table 2.

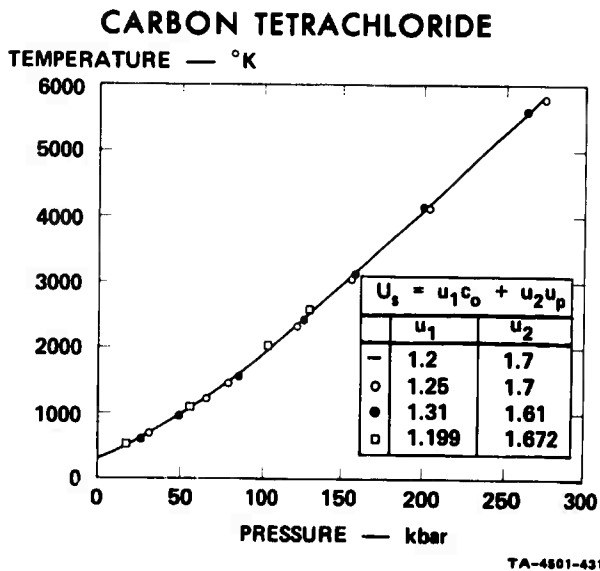


FIGURE 10 SHOCK TEMPERATURE FOR CARBON TETRACHLORIDE. Sensitivity of the calculated temperatures to the form of the Hugoniot. The input data are in Table 2.

starts to break down at high pressures, it holds well at low and moderate pressures and is a reasonable approximation.

If  $(\partial p/\partial T)_V$  is a function of volume only, then it follows that  $C_V$  is a function of temperature only. At atmospheric pressure and around room temperature for carbon tetrachloride and similar liquids,  $C_V$  increases with temperature. Bridgman<sup>10</sup> showed that at temperatures up to about 450°K,  $C_V$  of 18 liquids did not vary much with pressure up to 100 kbar.

#### E. The $C_V(T)$ Model

From the preceding sections, two main conclusions emerge concerning the shock temperature calculated by the Walsh-Christian method. First, the calculated temperature is more sensitive to variation of  $C_V$  than of  $(\partial p/\partial T)_V$ . Second, as the temperature and pressure increase along the Hugoniot, it seems likely that  $(\partial p/\partial T)_V$  will at first increase, then will decrease, whereas it is probable that  $C_V$  will increase. In attempting to develop a better equation of state, we have chosen to retain the Walsh-Christian assumption that  $(\partial p/\partial T)_V$  is constant, because the shock temperature is less sensitive to  $(\partial p/\partial T)_V$  than to  $C_V$ , because the increase and subsequent decrease of  $(\partial p/\partial T)_V$  will tend to cancel and, most important of all, we have little intuition as to the variation of  $(\partial p/\partial T)_V$ .

On the other hand, the calculated shock temperature is more sensitive to  $C_V$  than  $(\partial p/\partial T)_V$  and, as it is likely that  $C_V$  will increase as the temperature and pressure are increased, it seems worthwhile to make some assumptions concerning the variation of  $C_V$  with temperature and pressure. From the discussion in the previous section it is a reasonable assumption that  $C_V$  will be a function of temperature only. Consider the heat capacity of an ideal gas. For polyatomic molecules, there is usually a big increase in  $C_V$  as the temperature is raised from room temperature to several thousand degrees Kelvin. The increase in  $C_V$  is due primarily to an increase in the vibrational heat capacity as the oscillators become more classical as  $1-(h\nu/kT)$  approaches unity. It has previously been assumed that the vibrational heat capacity has the same value in

the liquid as in the ideal gas.<sup>11</sup> Therefore we have assumed that

$$C_v(T)_l = C_v(298)_l + \Delta C_{vg}^0$$

where  $C_v(T)_l$  is  $C_v$  of the liquid at  $T$ ,  $C_v(298)_l$  is  $C_v$  of the liquid at 298°K and  $\Delta C_{vg}^0$  is the increase in  $C_v$  of the ideal gas from 298°K to  $T$ . Because  $C_v$  and  $C_p$  of an ideal gas differ only by  $R$ , it follows that  $\Delta C_{vg}^0 = \Delta C_{pg}^0$ .

A computer program was written to integrate the differential Eq. (7) by a Runge-Kutta technique. If  $C_v$  and  $(\partial p/\partial T)_v$  are constant, then the Runge-Kutta method should give the same result as the trapezoidal integration of Eq. (8). This was checked for carbon tetrachloride, the temperatures calculated by the two methods agreeing to better than 1%.

#### F. Results of Temperature Calculations

Shock temperatures were calculated for carbon tetrachloride, nitromethane, and water.

##### 1. Carbon Tetrachloride

The shock temperature of carbon tetrachloride was calculated using  $C_v(T)$  and other input data as described in Table 7. The results, shown in Fig. 8, show much better agreement with the experimental measurements than do the temperatures calculated using the constant value of  $C_v$ . Mader<sup>12</sup> obtained good agreement with the experimental results using the Walsh-Christian method (constant  $C_v$ ). However, the agreement is fortuitous because he used the value of  $C_p$  for  $C_v$  (0.198 cal mole<sup>-1</sup> deg<sup>-1</sup> instead of 0.141 cal mole<sup>-1</sup> deg<sup>-1</sup>).

It is interesting to note that the experimentally observed temperatures start to diverge from those calculated using  $C_v(T)$  at pressures above about 150 kbar. This is the region in which Dick<sup>6</sup> observed a break in the  $p$ - $v$  Hugoniot and is also the region where Mader<sup>13</sup> calculated that significant amounts of decomposition of  $CCl_4$  into  $C_2Cl_6$  and  $Cl_2$  take place.

## 2. Nitromethane

Figure 11 shows the temperatures calculated for nitromethane using constant  $C_v$  and  $C_v(T)$ . The input data are in Table 7. The results are compared with those calculated by Enig and Petrone<sup>14</sup> using another equation of state. From their equation of state, Enig and Petrone obtained  $C_v$  as a function of temperature. The value of  $C_v$  at 298<sup>o</sup>K that they obtained (0.24 cal g<sup>-1</sup> deg<sup>-1</sup>) is significantly different from the literature value (0.29 cal g<sup>-1</sup> deg<sup>-1</sup>). More important, at about 2000<sup>o</sup>K,  $C_v$  was still increasing sharply and had a value of greater than 2 cal g<sup>-1</sup> deg<sup>-1</sup> whereas, as Jacobs<sup>15</sup> pointed out, the classical maximum for an ideal gas is  $3nR/M = 0.7$  where  $n$  is the number of atoms,  $R$  is the gas constant and  $M$  is the molecular weight.

At 86 kbar, Campbell, Davis, and Travis<sup>16</sup> have calculated a shock temperature of 1140<sup>o</sup>K from  $T = 300 + \Delta e/C_v$ , where  $\Delta e$  is the increase in internal energy across the shock. The apparent agreement with the temperature calculated by us using the Walsh-Christian method (Fig. 11) is fortuitous as Campbell, Davis, and Travis used the value of  $C_p$  for  $C_v$ . If the value of  $C_v$  is used, the shock temperature calculated from this equation of state becomes 1450<sup>o</sup>K.

Also at 86 kbar, Mader<sup>17</sup> calculated a shock temperature of 1168<sup>o</sup>K using the Walsh-Christian method, in apparent agreement with the results of similar calculations in Fig. 11. However this agreement is also fortuitous. Mader used  $C_p$  instead of  $C_v$  but the expected difference in calculated shock temperature was exactly offset by a 2.5-fold difference in the values used for  $(\partial p/\partial T)_v$ .

The lower temperatures calculated for nitromethane using  $C_v(T)$  imply that the rate of decomposition of nitromethane at high pressures is considerably faster than that expected from homogeneous thermal explosion theory using the rates measured at low pressures.

## 3. Water

In many ways water is an anomalous liquid. For this reason we have not attempted to estimate the variation of  $C_v$  with temperature.

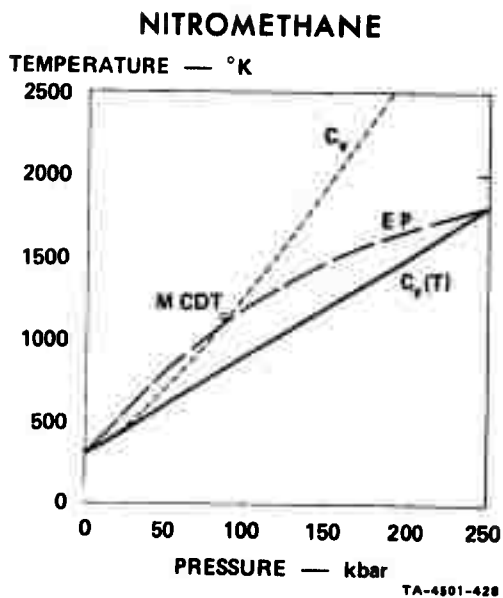


FIGURE 11 SHOCK TEMPERATURE FOR NITROMETHANE. The input data are in Table 2.

In Fig. 12 we report the results of calculations using the Walsh-Christian method and constant  $C_v$  and  $(\partial p/\partial T)_v$ . The results are compared with those calculated by Rice and Walsh<sup>5</sup> who assumed  $p$  to be constant and  $(\partial H/\partial V)_p$  to be a function of pressure only. From the analysis of the sensitivity of the Walsh-Christian method to  $C_v$  and  $(\partial p/\partial T)_v$  we have concluded that the shock temperature will be very sensitive to the value chosen for  $C_v$ . The observed difference between the present results and those obtained by Rice and Walsh is therefore regarded as not significant.

As found for carbon tetrachloride, shock temperature is not sensitive to the form of the  $p$ - $v$  Hugoniot, although the  $p$ - $v$  Hugoniots may be significantly different (Fig. 13).

#### G. Conclusions

The present method for calculating shock temperature takes better account of the properties of liquids and the greater dependence of shock temperature on  $C_v$  than on  $(\partial p/\partial T)_v$ . It is therefore considered to be an improvement on the Walsh-Christian method and will yield more realistic values of shock temperature in liquid explosives. This conclusion is substantiated by the improved agreement between calculated and experimental temperatures for carbon tetrachloride.

#### H. Future Work

Work on shock initiation is nearing completion. The new equation of state discussed in this report will be used to calculate shock temperatures in the difluoramino compounds for theoretical calculation of reaction times.

In the field of detonation failure, we plan to investigate the stability-structure problem in the difluoramino liquids giving particular emphasis to failure-wave pressure measurements and studies of detonation wave structure.

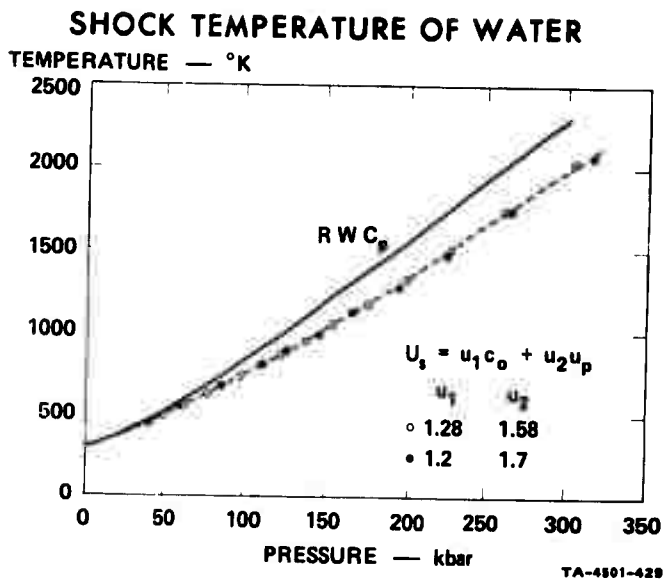


FIGURE 12 SHOCK TEMPERATURE FOR WATER. Comparison of the constant  $C_v$  model with the Rice-Walsh<sup>5</sup> constant  $C_p$  model. The shock temperatures calculated using the constant  $C_v$  model are not sensitive to the form of the Hugoniot. The input data are in Table 2. See also Figure 13.

#### Acknowledgments

We wish to thank L. B. Seely for introducing us to the problem and for his encouragement at all stages of the work. We are indebted for many helpful discussions to C. L. Mader, R. D. Dick, S. J. Jacobs, J. Enig, E. Bain, and R. F. Chaiken.

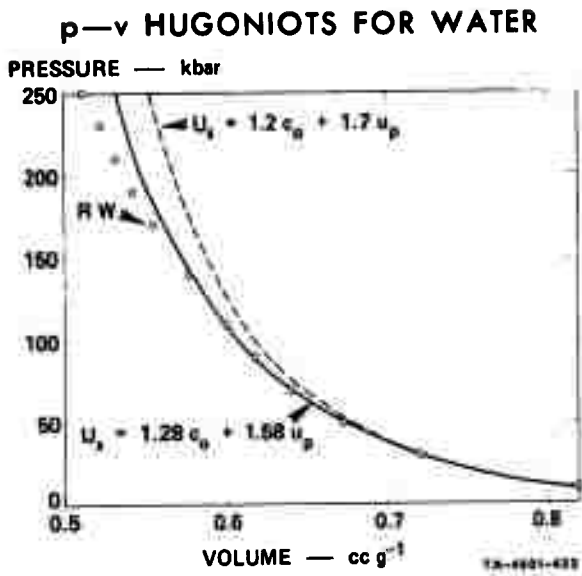


FIGURE 13 COMPARISON OF SHOCK HUGONIOTS FOR WATER CALCULATED FROM THE "UNIVERSAL HUGONIOTS" WITH THE EXPERIMENTAL VALUES MEASURED BY RICE AND WALSH<sup>5</sup>. The input data are in Table 2. See also Figure 12.

Table 6

COMPARISON OF SHOCK TEMPERATURES FOR CARBON TETRACHLORIDE  
 CALCULATED FROM EQ. (7) BY TRAPEZOIDAL EVALUATION OF THE INTEGRAL  
 AND SHOCK TEMPERATURES CALCULATED BY A RUNGE-KUTTA INTEGRATION OF EQ. (6)

p	v	T Equation (7) Trapezoidal	T Equation (6) Runge-Kutta
kbar	cc g <sup>-1</sup>	°K	°K
0	.631	298	298
29	.431	661	662
49	.401	980	980
73	.381	1401	1402
113	.361	2198	2198
144	.351	2866	2867
188	.341	3857	3857
253	.331	5385	5386

Table 7

INPUT DATA FOR CALCULATING SHOCK T

		$C_v$ fit*						Mol wt	$(\partial p/\partial T)_v$	Sound Speed	Specific Volume at $p=0$
		Constant	$CB/T^2$	$CC/T$	$CD$	$CE \times T$	$CF \times T^2$				
Units		cal mole <sup>-1</sup> deg <sup>-1</sup>							$10^{-7}$ dynes cm <sup>-2</sup> deg <sup>-1</sup>	$10^{-5}$ cm sec <sup>-1</sup>	cc g <sup>-1</sup>
Abbreviation for Runge-Kutta Computer Program		CA	CB	CC	CD	CE	CF	CM	DPDT	CO	VO
Carbon Tetrachloride	(1)	21.7	0	0	0	0	0	153.84	1.14	.926	.631
	(2)	19.53	0	0	0	0	0	153.84	1.14	.926	.631
	(3)	21.7	0	0	0	0	0	153.84	1.254	.926	.631
	(4)	21.7	0	0	0	0	0	153.84	1.14	.926	.631
	(5)	21.7	0	0	0	0	0	153.84	1.14	.926	.631
	(6)	21.7	0	0	0	0	0	153.84	1.14	.926	.631
	(7)	21.7	-75415.8	-2109.31	8.10247	-8.64548	1.12516	153.84	1.14	.926	.631
						$\times 10^{-4}$	$\times 10^{-7}$				
Nitromethane	(8)	17.8	0	0	0	0	0	61	1.637	1.30	.884
	(9)	17.8	1.23375	-9956.86	17.3573	8.09421	2.24624	61	1.637	1.30	.884
			$\times 10^6$			$\times 10^{-3}$	$\times 10^{-6}$				
Water	(10)	14.07	0	0	0	0	0	18.02	4.04	1.48	1.002
	(11)	14.07	0	0	0	0	0	18.02	4.04	1.48	1.002

$$* C_v = CA + (CB/T^2) + (CC/T) + CD + (CE \times T) + (CF \times T^2) / CM$$

Sources of Data: Carbon Tetrachloride:  $C_v$  (Ref. 9);  $C_v$  fit (Ref. 18);  $(\partial p/\partial T)_v$  (Ref. 9); Sound Speed (Ref. 19); Specific Volume (Ref. 9); Hugoniot 1.2, 1.7 (Ref. 2); 1.31, 1.61 (Ref. 8); 1.25, 1.7 (Ref. this work, arbitrary variation of  $u_1$ ); 1.199, 1.672 (Ref. 7)

Nitromethane:  $C_v$  (Ref. 20);  $C_v$  fit (Ref. 21);  $(\partial p/\partial T)_v$  calculated from  $(\partial p/\partial T)_v = \alpha C_v c_p^2 / v_0 C_p$ , where  $\alpha$  is the coefficient of expansion and  $C_p$  is the specific heat and constant pressure (Ref. 20); Sound Speed (Ref. 20); Specific Volume (Ref. 20); Hugoniot (Ref. 2)

Water:  $C_v$ ,  $(\partial p/\partial T)_v$ , sound speed, and specific volume (Ref. 22); Hugoniot 1.2, 1.7 (Ref. 2); 1.28, 1.58 (Ref. 2)

A

Table 7  
 CALCULATING SHOCK TEMPERATURES

Specific Volume at p = 0	Constants for Universal Hugoniot			Temp at p = 0 and v = 0	Second Volume Point on Hugoniot	First Volume Point on Hugoniot	Temp at First Volume on Hugoniot	
	$U_s = u_1 c_0 + u_2 u_p$	$U_1$	$U_2$					
cc g <sup>-1</sup>			°K	cc g <sup>-1</sup>	cc g <sup>-1</sup>	cc g <sup>-1</sup>	°K	
v0	U1	U2	T0	xE	C	Y[1]		
.631	1.2	1.7	298	.621	.631	298	Constant $C_v$ in Fig. 8; original in Fig. 9; Tables 6, 8, and 9 10% decrease in $C_v$ in Fig. 9; Table 8 10% increase in $(\partial p/\partial T)_v$ in Fig. 9; Table 8 Effect of p-v Hugoniot Fig. 10 and Table 9 $C_v(T)$ in Fig. 8	
.631	1.2	1.7	298	.621	.631	298		
.631	1.2	1.7	298	.621	.631	298		
.631	1.31	1.61	298	.621	.631	298		
.631	1.25	1.7	298	.621	.631	298		
.631	1.199	1.672	298	.621	.631	298		
.631	1.2	1.7	298	.621	.631	298		
.631	1.2	1.7	298	.621	.631	298		
.884	1.2	1.7	298	.874	.884	298	Constant $C_v$ in Fig. 11 $C_v(T)$ in Fig. 11	
.884	1.2	1.7	298	.874	.884	298		
1.002	1.2	1.7	293	.809	.819	323	Figs. 12 and 13 Figs. 12 and 13	
1.002	1.28	1.58	293	.809	.819	323		

work,  
 re  
 .28, 1.58 (Ref. 23)

B

**BLANK PAGE**

Table 8

SENSITIVITY OF THE SHOCK TEMPERATURE OF CARBON TETRACHLORIDE  
TO THE VALUES OF  $C_v$  and  $(\partial p/\partial T)_v$

P	v	$bT_B(V_0 - V_1)$	$bI/2C_r$	$T_H - T_B$	R	$\frac{\Delta T_{C_v}}{\Delta T (\partial p/\partial T)_v}$ calc. analytically	$\frac{\Delta T_{C_v}}{\Delta T (\partial p/\partial T)_v}$ obs. empirically
kbar	cc g <sup>-1</sup>	deg.	deg.	deg.	g cc <sup>-1</sup>		
0	.631	0	0	0	-	-	-
29	.431	169	98	223	3.6	1.8	2.4
49	.401	207	150	515	4.7	2.4	3.4
73	.381	233	208	978	6.2	3.2	4.5
113	.361	262	274	1696	8.0	4.1	5.7
144	.351	277	300	2354	9.8	5.1	7.0
188	.341	292	328	3335	12.4	6.4	8.3
253	.331	308	347	4853	16.3	8.4	9.7

Input data used: See Table 7

Table 9

## P-v HUGONIOTS FOR CARBON TETRACHLORIDE CALCULATED FROM

$$U_g = u_1 c_0 + u_2 u_p$$

$u_1 =$ $u_2 =$ $v$ cc g <sup>-1</sup>	1.2 1.7 p kbar	1.25 1.7 p kbar	1.31 1.61 p kbar	1.199 1.672 p kbar
.631	0	0	0	0
.431	29	32	31	28
.401	49	54	50	47
.381	73	79	70	68
.361	113	122	103	103
.351	144	156	127	130
.341	188	204	158	
.331	253	275	202	

In all cases  $c_0 = .926 \times 10^5$  cm sec<sup>-1</sup>.

## References

1. J. M. Walsh and R. H. Christian, *Phys. Rev.*, 97, 1554 (1955).
2. I. M. Voskoboinikov and B. M. Bogomolov, *ZhETF Pis'm a* 7, 338 (1968).
3. Personal communication from C. L. Mader re experiments by Ramsay.
4. M. Cowperthwaite, *Amer. J. Phys.*, 34, 1025 (1966).
5. M. H. Rice and J. M. Walsh, *J. Chem. Phys.* 26, 824 (1957).
6. R. D. Dick, LA-3915, Los Alamos Scientific Laboratory of the University of California, Los Alamos, New Mexico.
7. Recalculated from Ref. 6 by R. D. Dick.
8. Stanford Research Institute Project 4051 Technical Progress Report 67-2 (Semiannual), "Sensitivity Fundamentals," October 1967.
9. D. Harrison and E. A. Moelwyn-Hughes, *Proc. Roy. Soc.* A239, 230 (1957).
10. P. W. Bridgman, The Physics of High Pressure, Bell and Sons, Ltd., London, 1958, pp. 127-142.
11. D. B. Davies and A. J. Matheson, *Disc. Farad. Soc.*, 43, 216 (1967).
12. C. L. Mader, personal communication.
13. C. L. Mader, Report No. LA-2900, Los Alamos Scientific Laboratory of the University of California, Los Alamos, New Mexico.
14. J. W. Enig and T. J. Petrone, *Phys. Fluids*, 9, 398 (1966).
15. S. J. Jacobs, personal communication.
16. A. W. Campbell, W. C. Davis, and J. R. Travis, *Phys. Fluids*, 4, 498 (1961).
17. C. L. Mader, quoted in Ref. 16.
18. JANAF Thermochemical Tables, Dow Chemical Company, Midland, Michigan.
19. Handbook of Chemistry and Physics, Chemical Rubber Publishing Co., Cleveland, Ohio, 49th Ed., 1968-9, p. E-38.
20. B. O. Reese, L. B. Seely, R. Shaw, and D. Tegg, submitted to *Jour. Chem. Eng. Data*.

21. J. P. McCullough, D. W. Scott, R. E. Pennington, I. A. Hossenlopp, and G. Waddington, Amer. Chem. Soc., 76, 4791 (1954).
22. N. E. Dorsey, Properties of Ordinary Water Substance, Reinhold, New York, (1940).
23. R. W. Woolfolk, personal communication.

## IV KINETICS AND MECHANISMS OF THERMAL DECOMPOSITION

(David S. Ross and M. E. Hill)

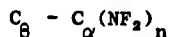
### A. Introduction

Our last report<sup>1</sup> presented a theoretical model for detonations in liquids in terms of the types of the chemical reactions available to the material in question. For NF materials, LVD was described as resulting from an exothermic chain reaction. HVD was proposed to be due to an exothermic unimolecular dehydrofluorination for materials such as 1,2-DP which are structurally capable of undergoing unimolecular loss of HF, and some unspecified reaction for materials such as 2,2-DP which cannot.

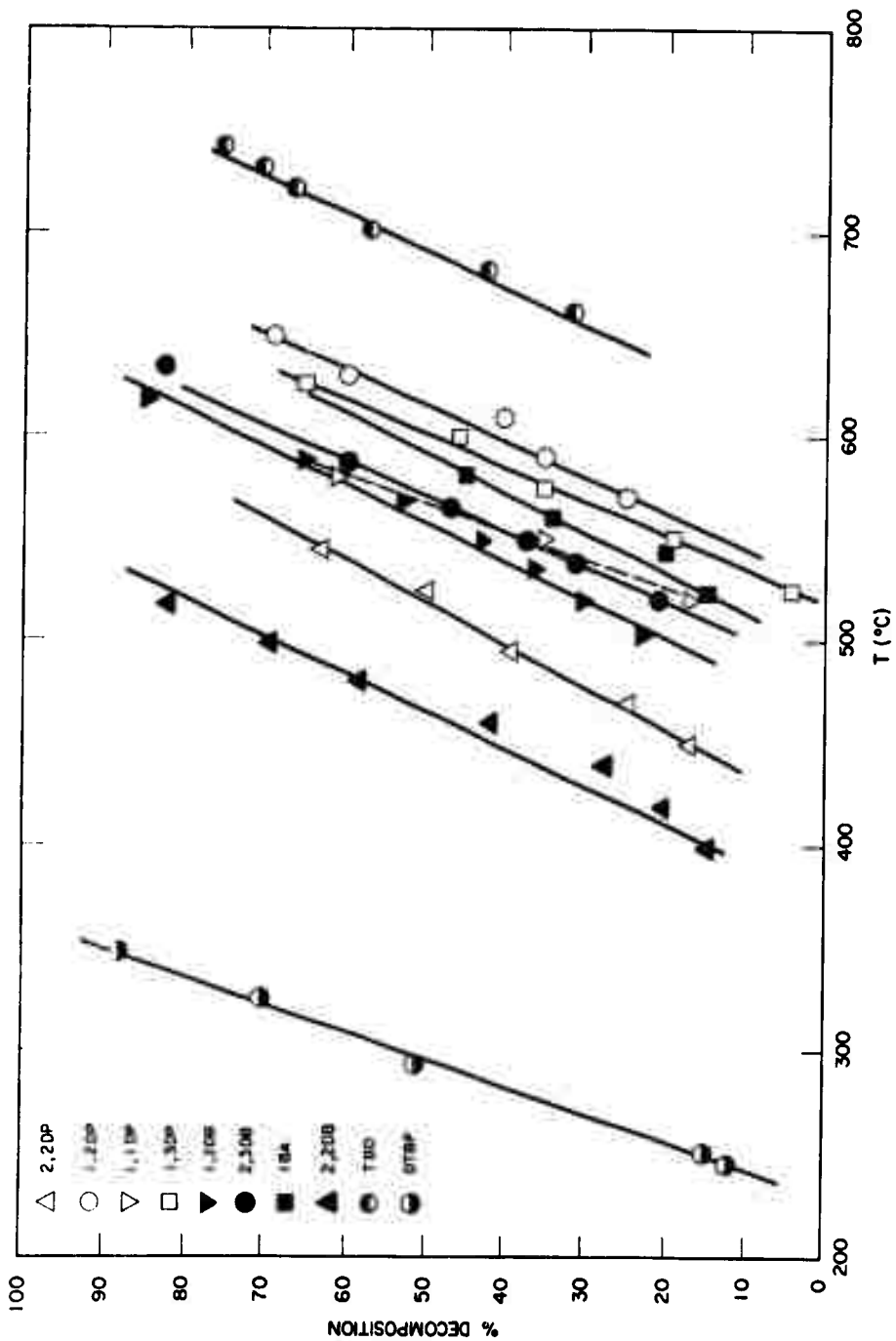
There is more to be done with the model in terms of refinements and further application to other explosive systems. However, we have delayed further work in this area to allow time for some laboratory work as well as for preparation of manuscripts on NF chemistry for publication. We will present below the final results on the very low pressure pyrolysis (VLPP) of NF compounds, as well as our introductory experiments with nitropropanes.

### B. VLPP of NF Materials

The VLPP's of t-butyldifluoramine (TBD) and 2,2-DB have been performed, and the complete set of VLPP data on NF materials is presented in Fig. 14. These results confirm our earlier discussion of structure and stability<sup>2</sup> in which we suggested that there are two factors which act to destabilize the compound



They are, first, geminate substitution ( $n > 1$ ), which lowers the activation energy toward decomposition, and, second,  $\beta$ -substitution, which raises

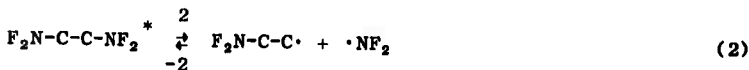
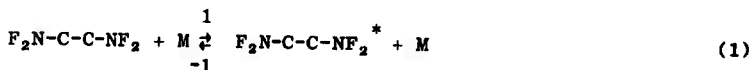


XTC-4051-326R

FIGURE 14 VLPP DATA FOR NF COMPOUNDS AND DTBP

the A factor for decomposition. 2,2-IB is destabilized through both processes, and thus as we had predicted,<sup>2</sup> is the least thermally stable material we have studied.

A discussion of the detailed mode of decomposition of vicinal bisdifluoramines entails consideration of the reaction from both directions. Thus the fact that propylene, butene-2, and isobutylene are produced as the overwhelmingly major products in the VLPP of 1,2-DP, 2,3-DP, and IBA respectively suggests that we are observing the reverse of the addition reaction of  $N_2F_4$  to these olefins. This addition has been studied by Dijkstra, Kerr, and Trotman-Dickenson<sup>3a,b,c</sup> (DKT), and a detailed mechanistic path for the reaction sequence based on both that work and ours is:



in which \* denotes a vibrationally excited state and M is a collision partner. Each step is written as reversible, however, depending upon the method and direction of study, certain steps proceed only in one direction in a practical sense. Thus, for example, Eq. (4) in the case of the work by DKT is truly reversible, whereas for this work, step 4 is very rapid but step -4, because of the low pressure, proceeds essentially at zero rate.

Figure 15 provides a schematized reaction coordinate for the sequence, and embodies the fact provided by DKT<sup>3b</sup> that the activation energies for 3 and -4 are the same to within 2 kcal/mole, and thus the  $C-NF_2$  bond strength in  $F_2N-C-C\cdot$  is small. They fall in the range

8-16 kcal/mole for the olefins studied, and the value used in Fig. 15 of ~14 kcal/mole is for propylene. Since  $k_1$  is small,  $v_2$  (the velocity of step 2)  $\gg v_{-1}$ , and thus step 1 is rate controlling. The experimental activation energy for vicinal bisdifluoramine (~ 55 kcal/mole) applies therefore to step 1. The heat value of ~ 20 kcal/mole for -5 is from the work of Piette, Johnson, Booman, and Colburn.<sup>4</sup>

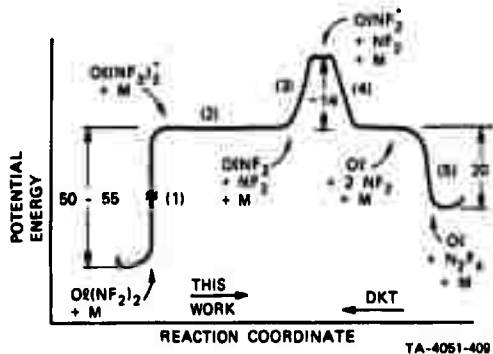


FIGURE 16 REACTION COORDINATE DIAGRAM FOR THE REACTION:  
 $C=C + N_2F_4 \rightleftharpoons F_2N-C-C-NF_2$

DKT showed that in their direction of study the slow step is -4, and while Fig. 15 suggests that both -4 and -5 are slow, in fact  $v_{-5} \gg v_{-4}$ . The reasoning here points to the need to be careful in interpreting reaction coordinate diagrams in that they show the enthalpy but not the entropy factors involved in the process. Thus at the temperatures and pressures of the DKT work

$$k_{-5} = 10^{13.5} \exp(-15,200/RT) \text{ l}/(\text{mol sec})^\ddagger$$

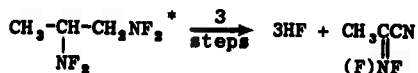
<sup>‡</sup>  $N_2F_4$ , under DKT conditions of a mean temperature of 90°C and pressures in the range 20 to 600 torr, is in its second order region,<sup>5</sup> and this expression is derived from  $k = 1.5 \times 10^{12} T^{0.5} \exp(-15,200/RT)$  liters/(mol sec)<sup>5</sup> for M = argon and with T = 400°K.

while

$$k_{-4} = 10^{7.6} \exp(-13,700/RT) \text{ l}/(\text{mol sec})$$

The activation energy terms are comparable, but the preexponential terms differ by about six powers of ten. In fact, under the DKT experimental conditions, Eq. (5) is a true equilibrium.

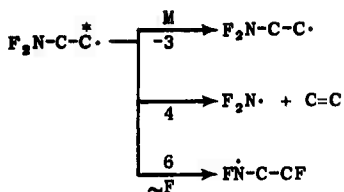
It is of interest to consider the events along the plateau of Eq. (2) in Fig. 15. Here the vibrationally excited species  $F_2N-C-C-NF_2^*$  is undergoing rapid internal exchanges of energy among the various modes available, and while in most cases a C-N bond is ultimately broken, there is another option available to the molecule. It has recently been shown that vibrationally excited  $CH_3NF_2$  loses HF yielding HCN.<sup>6</sup> Thus, it is conceivable that such a process is taking place here in the case of 1,2-DP, for example,



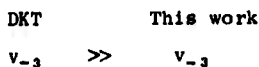
which would explain the presence of N-fluoriminopropionitrile in the product mixture from that compound. The  $SiF_4$  would then arise from the well known reaction of HF with glass



Lesser products from the VLPP of 1,2-DP, such as  $CH_3CN_3$ ,  $FCH_2CN$ , and  $CH_3NF_3$  can be explained by considering the fact that the effects of pressure on the DKT kinetics of  $N_2F_4$  addition to olefins suggested that the vibrationally excited species  $FN_2-C-C^*$  has some finite lifetime (as opposed to being a transient intermediate). In view of our isolating a material with a C-F bond, we propose that there is a route available to the excited radical in addition to -3 and 4, namely internal migration of fluorine from nitrogen to carbon.

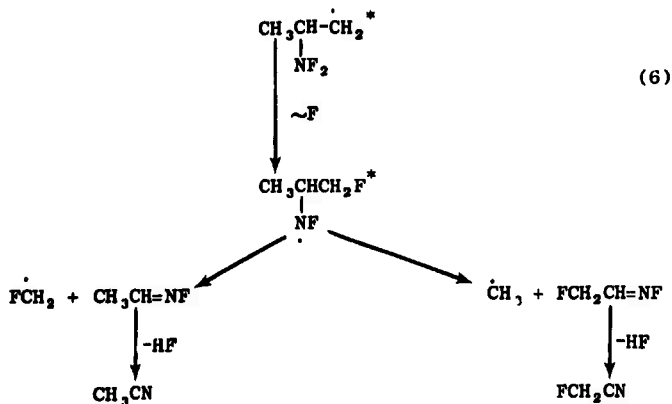


This process has adequate driving force as it is some 35-45 kcal/mole exothermic, and since DKT operated at pressures in the 20 to 600 torr range while this work was performed at less than  $10^{-3}$  torr,

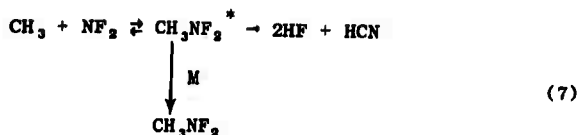


Thus 6 is observable in our work whereas it was not in that by DKT.

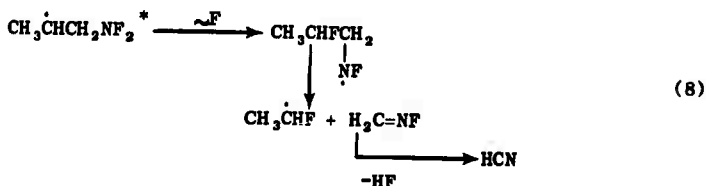
Thus, for the VLPP of 1,2-DP the following scheme is proposed to account for the minor products outside of the already explained N-fluoriminopropionitrile:



The methyl radicals are accounted for in the observation of  $\text{CH}_3\text{NF}_2$  and  $\text{HCN}^6$



The same process for the fragment  $\text{CH}_3\dot{\text{C}}\text{HCH}_2\text{NF}_2^*$



must take place, however, the product  $\text{H}_2\text{C}=\text{NF}$  has not been detected, and the small amount of HCN observed can be accounted for by Eq. (7). One explanation for this observation is that the secondary radical in 8 is 2-3 kcal/mole more stable than the primary radical in 6, 7 and thus the latter should undergo rearrangement more rapidly than the former.

Of course, it is possible to explain the formation of all of the minor products by wall reactions. In fact, we have evidence that 1,2-DP does dehydrofluorinate readily through a surface-catalyzed process to yield N-fluoriminopropionitrile.<sup>8</sup> However, since there are plausible homogeneous routes leading to the observed products, we prefer to suggest them as the route of formation.

### C. VLPP of Nitro Materials

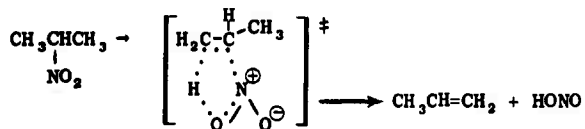
VLPP's of both 1- and 2-nitropropane (1-NP and 2-NP) have been reported by Spokes and Benson.<sup>9</sup> We are repeating the work for the sake of completion as a prelude to our study of the dinitropropanes. Spokes and Benson using a 9,000 collision vessel found that the nitropropanes decompose with the following high pressure rate parameters

$$k_{1\text{-NP}} = 10^{11.6 \pm 0.6 - (4.2 \pm 2)/\theta} \text{ sec}^{-1}$$

and

$$k_{2\text{-NP}} = 10^{11.3 \pm 0.2 - (4.0 \pm 0.5)/\theta} \text{ sec}^{-1}$$

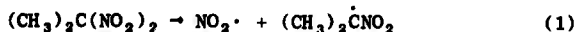
( $\theta = 2.303 RT \times 10^3 \text{ kcal/mole}$ ) via a 5-center transition state, eliminating  $\text{HNO}_2$  in a concerted fashion and yielding propylene. Thus, for example, the VLPP of 2-NP proceeds as follows:



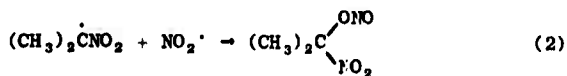
We have studied 1-NP in a 100 collision vessel and have found a  $T_{1/2}$  of  $665^\circ\text{C}$ . Propylene, as expected, is the single observed product. While  $\text{HNO}_2$  cannot be seen under our gas chromatographic conditions, it is most likely present. 2-NP is currently being studied.

The study of the dinitropropanes (DNP) is expected to be complicated by the fact that these materials have rather low vapor pressures at room temperature. Thus at  $25^\circ\text{C}$  1,1-DNP and 2,2-DNP have vapor pressures well below 1 torr, and a vapor pressure convenient for VLPP operation of 5 to 10 torr is attainable only at temperatures of  $70$  to  $80^\circ\text{C}$ .<sup>10</sup> The sample volume of the reactor will have to be heated to this temperature to allow the study to proceed, and we are currently considering various possible ways of doing this.

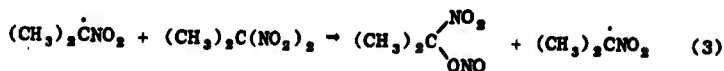
The thermal decomposition of 2,2-DNP from  $175$  to  $210^\circ\text{C}$  has been studied by Flournoy<sup>11</sup> and in that work he observed equimolar proportions of acetone,  $\text{NO}$ , and  $\text{NO}_2$  as products. The proposed mechanism involved initial scission of the CN bond



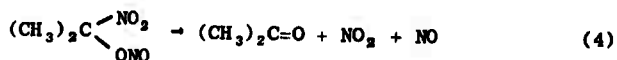
followed by formation of an intermediate nitronitrite by either recombination



or by displacement on another molecule of 2,2-DNP



The final step in the formation of acetone is proposed as the rapid decomposition of the nitronitrite

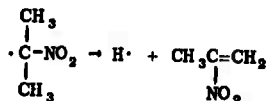


The rate of disappearance of 2,2-DNP followed the rate law

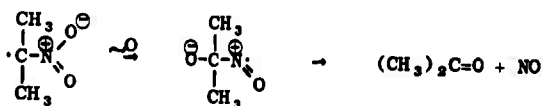
$$k_{2,2\text{-DNP}} = 10^{18.5-50/\theta} \text{ sec}^{-1}$$

which was applied to the slow step (1)

A comparison of the constants  $k_{2\text{-NP}}$  and  $k_{2,2\text{-NP}}$  shows that for the case of geminate materials C-N scission will be faster than HONO elimination above 300°K. The VLPP study of 2,2-DNP should prove interesting since VLPP operation is at such low pressure, the rate of either step 2 or step 3 should be vanishingly small, and thus we should see the products resulting from the decomposition of the radical intermediate,  $(\text{CH}_3)_2\dot{\text{C}}\text{NO}_2$ . For this process there are two possible pathways. First, by analogy to the decomposition of t-butyl radical in our reactor,<sup>12</sup> the intermediate could lose a hydrogen atom to yield 2-nitropropene



Second, an intramolecular oxygen rearrangement may take place to yield, subsequently, acetone and NO.



This second possibility, by the way, coming after initial loss of  $\text{NO}_2$ , would provide equimolar quantities of acetone, NO, and  $\text{NO}_2$ , and thus is an alternate explanation of Flournoy's results.

#### D. Future Work

Woolfolk has presented an approach to correlating LVD gap sensitivity to thermochemical stability (see Section II). His reaction heat values ( $\Delta H_r$ ) are defined by the process whereby the liquid explosive goes to thermodynamically favored end products such as HF, C, and  $\text{N}_2$ . While at this point such a definition for  $\Delta H_r$  is all that is reasonably available, it is not clear that in an LVD process such products are indeed formed. For example, since the temperature in LVD may never exceed  $1000^\circ\text{C}$ , it is possible that less stable (in a thermodynamic sense) materials such as olefins, imines, and nitriles, are "trapped," in that kinetically they cannot proceed to the aforementioned end products.

Were some measure of the degree of the thermodynamic inefficiency known for the LVD process, a correction could be applied to the  $\Delta H_r$  values, and a firmer correlation would be the result. In this regard we have discussed the possibility of carrying out LVD on a small scale in some sort of enclosure such that the products of the explosion could be trapped and characterized. Particularly interesting would be the possibility of finding products in these proposed experiments that have been also seen in the VLPP studies on the same compounds. Thus, for example, the presence of  $\text{FCH}_2\text{CN}$  as one of the end products of the LVD of 1,2-DP would verify our supposition<sup>13</sup> that the highly exothermic migration of fluorine from nitrogen to carbon as observed by VLPP plays an important role in the detonation process.

## References

1. Stanford Research Institute Project 4051, Technical Progress Report 68-2 (Semiannual), "Sensitivity Fundamentals," September 15, 1968.
2. Stanford Research Institute Project 4051, Technical Progress Report 68-1 (Semiannual), "Sensitivity Fundamentals," March 15, 1968.
3. (a) A. J. Dijkstra, J. A. Kerr, and A. F. Trotman-Dickenson, J. Chem. Soc., (A), 582 (1969); (b) ibid., 105 (1967); (c) ibid., 864 (1967).
4. L. Piettle, F. Johnson, K. Booman, and C. Colburn, J. Chem. Phys. 35, 1481 (1961).
5. A. Modica and D. Hornig, J. Chem. Phys., 49, 629 (1968).
6. C. Bungardner, E. Lawton, and H. Carmichaels, Chem. Comm., 1079 (1968).
7. S. W. Benson, Thermochemical Kinetics, John Wiley and Sons, Inc., New York, 1968, p. 215.
8. Stanford Research Institute Project 4051, Technical Progress Report 64-2 (Annual), "Sensitivity Fundamentals," March 14, 1964, p. 81.
9. G. N. Spokes and S. W. Benson, J. Amer. Chem. Soc., 89, 6030 (1967).
10. D. E. Holcomb and D. C. Dorsey, Jr., Ind. and Eng. Chem., 41, 2788 (1949).
11. J. M. Flournoy, J. Chem. Phys., 36, 1107 (1962).
12. Stanford Research Institute Project 4051, Technical Progress Report 67-1 (Semiannual), "Sensitivity Fundamentals," March 15, 1967, p. 62.
13. Stanford Research Institute Project 4051, Technical Progress Report 66-2 (Annual), "Sensitivity Fundamentals," March 15, 1966, p. 64.

APPENDIX: PAPERS AND PRESENTATIONS PREPARED  
DURING THIS REPORT PERIOD

- J. G. Berke and L. B. Seely, "Equation of State of Polydiethylene Glycol-Bis-Allyl Carbonate," accepted for publication in AIAA Journal, publication date June 1969.
- M. Cowperthwaite, L. B. Seely, and R. Shaw, "Calculation of Shock Temperatures in Liquid Explosives Using the Walsh-Christian Method," paper presented by R. Shaw at Western States Section--The Combustion Institute, April 1969, at U.S. Naval Weapons Center, China Lake, California. Abstract to be published in Combustion and Flame.
- M. Cowperthwaite and R. Shaw, "Calculation of the Shock Temperature of Liquids," submitted to J. Chem. Phys. in May 1969.
- B. O. Reese, L. B. Seely, D. Tegg, and R. Shaw, "Heat Capacity at Constant Volume of Nitromethane, Liquid TNT, and Four Difluoraminoalkanes," accepted for publication in J. Chem. Eng. Data, publication date December 1969.
- D. Ross, T. Mill, and M. E. Hill, "The VLPP of NF Compounds. I. t-BuNF<sub>2</sub>," submitted to J. Amer. Chem. Soc.
- D. Ross, T. Mill, and M. E. Hill, "The VLPP of NF Compounds. II. 1,2- and 2,2-Bis-difluoramino propane," in preparation.
- D. Ross, D. Tegg, and M. E. Hill, "The VLPP of NF Compounds. III. Kinetics of Unimolecular Decomposition of Bis-difluoraminoalkanes," in preparation.
- D. Ross and R. Shaw, "Unimolecular Dehydrofluorination of Methyl difluoramine," accepted for presentation at ACS Meeting in New York City, September 1969.
- R. Shaw, "Heat Capacity of Liquids. Estimation of Heat Capacity at Constant Pressure and 25°C Using Additivity Rules," accepted for publication J. Chem. Eng. Data, publication date October 1969.
- R. Shaw, "High Pressure Kinetics. Decomposition of Liquid Explosives (Nitromethane, Methyl Nitrite, and some Bis-Alkyl-Difluoramines) in the 100 kbar Region," to be presented at the ACS Meeting in New York City, September 1969.
- R. W. Woolfolk and A. B. Amster, "Low-Velocity Detonation: Some Experimental Studies and the Interpretation," Proceedings Twelfth International Symposium on Combustion, Poitiers, France (1968), in press.
- R. W. Woolfolk, "Low-Velocity Detonation" presented before the ICRPG Meeting on Solid Propulsion, April 12, 1969, Huntsville, Alabama.

UNCLASSIFIED

Security Classification

DOCUMENT CONTROL DATA - R & D

Security classification of title, body of abstract and indexing annotation must be entered when the overall report is classified

1. ORIGINATING ACTIVITY (Corporate author) Stanford Research Institute 333 Ravenswood Avenue Menlo Park, California 94025		2a. REPORT SECURITY CLASSIFICATION <b>UNCLASSIFIED</b>	
		2b. GROUP N/A	
3. REPORT TITLE  SENSITIVITY FUNDAMENTALS			
4. DESCRIPTIVE NOTES (Type of report and inclusive dates) Semiannual Technical Progress Report 69-1 (September 16, 1968 to March 15, 1969)			
5. AUTHOR(S) (First name, middle initial, last name) Marion E. Hill                      Derek Tegg                      David S. Ross Robert W. Woolfolk              Robert Shaw Hans R. Bredfeldt                Michael Cowperthwaite			
6. REPORT DATE May 31, 1969		7a. TOTAL NO. OF PAGES 88	7b. NO. OF REFS 54
8a. CONTRACT OR GRANT NO. Nonr 3760(00)		9a. ORIGINATOR'S REPORT NUMBER(S)  69-1	
b. PROJECT NO. PRU 4051		9b. OTHER REPORT NO(S) (Any other numbers that may be assigned this report)	
c.		d.	
10. DISTRIBUTION STATEMENT  Qualified requestors may obtain copies of this report from DDC.			
11. SUPPLEMENTARY NOTES		12. SPONSORING MILITARY ACTIVITY  Office of Naval Research Washington, D.C.	
13. ABSTRACT  Under the sponsorship of the Office of Naval Research, Stanford Research Institute is studying the following fundamental sensitivity properties of difluoro-amino compounds: <ol style="list-style-type: none"> <li>1. The low-velocity detonation (LVD) wave characteristics of the liquid phase.</li> <li>2. The relation of shock sensitivity and failure diameter to the flow and the chemical reaction rate behind the shock front.</li> <li>3. The mechanism and kinetics of thermal decomposition of the compounds in the gas phase.</li> </ol> <p>The compounds chosen for this study are as simple as possible structurally, but at the same time they have physical properties that permit their use in each phase of the study. The model compounds are the bis difluoroamino and tris difluoroamino isomers of the propane series--primarily 1,2- 1,3-, 1,1-, and 2,2-bis(difluoroamino)propane (1,2-, 1,3-, 1,1-, and 2,2-DP); 1,2-bis(difluoroamino)-2-methyl propane (IBA); 2,3-bis(difluoroamino)butane, (2,3-DB) in meso and <u>dl</u> forms; 1,2,2-tris(difluoroamino)propane (1,2,2-TP); and 2,3,3-tris(difluoroamino)butane (2,3,3-TB). These compounds are being used so that the results from each experimental technique can be interrelated without having to account for effects caused by different functional groups, amount of carbon content, and chain branching. Through the use of isomers, structural effects on the results from a particular technique can be determined--for example, the differences in the effect of vicinal</p>			

DD FORM 1473 (PAGE 1)

NOV 68 57/ 0101-807-6801

UNCLASSIFIED

Security Classification

14 KEY WORDS	LINK A		LINK B		LINK C	
	ROLE	WT	ROLE	WT	ROLE	WT
<p><b>Sensitivity</b></p> <p><b>NF Compound Sensitivity</b></p> <p><b>1,2-Bis(difluoramino)propane</b></p> <p><b>2,3-Bis(fluorimino)butane, geometric isomers</b></p> <p><b>t-butyl difluoramine</b></p> <p><b>2,3-bis(difluoroamino)butanes, diastereoisomers</b></p> <p><b>1-difluoraminobutane</b></p> <p><b>2-difluoraminobutane</b></p> <p><b>2-difluoramino-2-methylpropionitrile</b></p> <p><b>2-fluorimino-3-difluoramino-3-methylbutane</b></p> <p><b>1,2-bis(difluoramino)-2-methylpropane</b></p> <p><b>N-fluoriminopropionitrile</b></p> <p><b>2,3-bis(difluoramino)-2-methylbutane (triemethyl-ethylene adduct)</b></p> <p><b><u>NF Compounds</u></b></p> <p><b>Low Velocity Detonation</b></p> <p><b>Critical Failure Diameter</b></p> <p><b>Detonation Reaction Times</b></p> <p><b>Solution Decomposition Kinetics</b></p> <p><b>HF Elimination</b></p> <p><b>Very Low-Pressure Pyrolysis</b></p> <p><b>Gap Sensitivity</b></p> <p><b>Radical Reactions</b></p> <p><b>Photocatalytic Decomposition</b></p>						

and geminate difluoramino groups on the ease of initiation and on the environmental stability of compounds containing them. A similar approach has begun with isomeric nitro compounds.

### Low-Velocity Detonation

The shock wave interactions that can lead to the initiation of low-velocity detonations (LVD) are examined with particular emphasis on cavitation. The two forms of cavitation, gas inclusion and pure vaporization, are discussed. The latter's relationship to the shock-wave interactions in the LVD gap sensitivity tests is examined. We believe that pure vaporization cavitation, which cannot be removed by degassing, is present under gap test conditions. Experimental studies in the gap test arrangement show the presence of cavitation in qualitative agreement with theoretical prediction.

The "universal Hugoniot" for liquids has been reevaluated using a temperature correction for the sonic velocity,  $c_0$ . The new equation is improved slightly over the one formerly used. This concluded the effort in this area.

A trace dye method for following the flow field behind a shock wave was studied. We concluded that this method was not suitable at present for our studies and work on it will be discontinued.

Experiments on the effect of confinement wall thickness on the LVD gap sensitivity are discussed and preliminary charge diameter studies are reported. A summary of the effects of confinement on the LVD gap sensitivity is presented.

Some of the physical and chemical properties of liquid explosives are correlated with the LVD gap sensitivity. This correlation is remarkably good considering its simplicity. The evidence that LVD initiation may be a gas phase phenomenon is discussed. This further supports the contention that LVD may be related to the formation of cavities in the liquid explosive.

### Physics and Chemistry of Detonation

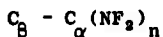
A new method for calculating shock temperatures in liquid explosives has been developed from the Walsh-Christian method for metals. The Walsh-Christian method assumes that  $C_v$  and  $(\partial p/\partial T)_v$  are constant. The basis of the present method is a variational analysis which shows that shock temperature is more sensitive to variations in  $C_v$  than to variations in  $(\partial p/\partial T)_v$ . Thus  $C_v$  is assumed to be a function of temperature and  $(\partial p/\partial T)_v$  is assumed to be constant. It is considered likely that  $C_v$  will increase with temperature due to an increase in the vibrational heat capacity. The simplest assumption is that  $C_v$  of the liquid will increase as  $C_v$  of the ideal gas. This is the basis of the  $C_v(T)$  model.

Shock temperatures of carbon tetrachloride and nitromethane have been calculated using both constant  $C_v$  and  $C_v(T)$ . Shock temperatures for carbon tetrachloride calculated using the  $C_v(T)$  model are in better agreement with experimental brightness temperatures than those calculated using the Walsh-Christian constant  $C_v$  model. Shock temperatures for nitromethane are compared with those of other workers.

Shock temperatures in water were calculated using constant  $C_v$  and  $(\partial p/\partial T)_v$ . The temperatures are about 15% less than those calculated by Rice and Walsh using a model based on constant  $C_p$ . This difference is not regarded as significant compared with the uncertainties in the variation of  $C_v$  and  $C_p$  with temperature and pressure.

#### Kinetics and Mechanisms of Thermal Decomposition

The VLPP studies of all the NF compounds we have had at hand have been completed, and the accumulated data suggest a model of unimolecular decomposition in which the  $NF_2$  compound



is destabilized by both  $\alpha$ - $NF_2$  substitution due to a decrease in  $E_a$ , and by  $\beta$ -alkyl or  $\beta$ - $NF_2$  substitution due to an increase in the A factor. Since both factors are operative in the case of 2,2-DB, it is thermally the least stable NF material we have studied.

A detailed reaction coordinate diagram may be constructed for the system  $F_2N-C-C-NF_2 \rightleftharpoons C=C + N_2F_4$  on the basis of both our work and that by Trotman-Dickenson. It is possible, on the basis of the diagram, to explain the side-products observed in the VLPP of 1,2-DP.

The VLPP of 1-nitropropane has been studied. The products are propylene and presumably HONO, and the  $T_{1/2}$  value is 665°C.